Autonomous Bicycle Project

Team Final Report by:
Sung Won An, Rannie Dong, Eric Huang, Jason Hwang,
Olav Imsdahl, Weier Mi, Arundathi Sharma, Rhett Wampler, Xiangyun (Joyce) Xu

Professor Andy Ruina
Biorobotics and Locomotion Lab
Mechanical and Aerospace Engineering, Cornell University

Fall 2015

Abstract

We are developing a robotic bicycle that we hope can balance better than any previous robotic two-wheeler (single-track vehicle). Many have tried using a variety of balance strategies, including gyroscopes and reaction wheels. Our bicycle will use only steering for balance, much like a human does. The mathematical model we use to develop our controller uses a point-mass model of the bicycle and bicycle rider. We also use simplified bicycle geometry with a vertical fork and no offset. The equations of such a bike are more manageable than the non-linear equations of a full bicycle. The eventual goal is to use massive computer optimization to find a steering strategy that maximizes the disturbances from which the bike can right itself. In the meantime we will see how well we can balance the bicycle using a steering angle rate (controlled by a motor) that is a linear function of the instantaneous steer angle, the bike lean angle, and the bike falling rate. When all put together, we hope to demonstrate the bike riding around Cornell campus on its own.

Contents

List of Figures

Acknowledgement

The author wishes to thank the University of Liverpool Computing Services Department for the development of this LaTeX thesis template.

Chapter 1

Review of Other Robotic Bicycles

Contributor: Sung Won An

1.1 Introduction

The concept of self-balancing two-wheeled vehicles dates back to 1911, in a work of fiction by Kenneth Brown titled, "Two Boys in a GyroCar", as shown in Fig.1.1. Since then, there have been numerous attempts to build a self-stabilizing two-wheeled vehicle. In 1912, Pyotr Shilovsky, a member of the Russian royal family, commissioned the Shilovski Gyrocar. The Wolseley Tool and Motorcar Company manufactured the design in Fig.1.2 in 1914, which weighed 2.75 tons and had a large turning radius. Since the 20th century, we have come much closer to realizing this goal. Today, there are a large variety of self-stabilizing bicycles and motorcycles that have been explored. These vehicles range from commercial bicycles that are available on the market to simple concepts that have never been built.

Figure 1.1: Two-wheeled self-balancing automobile concept described in *2 Boys in a GyroCar*.[1]

All self-stabilizing two-wheeled vehicles can be grouped into three categories based on the specific method by which the vehicle achieves balance. These categories are: balance by gyroscope, balance by reaction wheel, and balance by steering. Many advances have already been made towards building highly stable vehicles that balance by gyroscope or by a reaction wheel. However, in the context of human interaction with a bicycle or motorcycle, gyroscopes and reaction wheels tend to be irrelevant. Our research group is interested in studying balance by steering to gain a better understanding the mechanisms by which we balance on bicycles. In this final category, the problem yet remains in building a sufficiently stable bicycle.

Figure 1.2: The Shilosky Gyrocar.[2]

[1]Kenneth Brown. Two Boys in a GyroCar. Digital image. Amazon. Web. 30 October 2015.

1.2 Balance by Gyroscope

The gyroscope category consists of vehicles that use a massive wheel that spins at high speeds in order to keep stable. This method exploits gyroscopic effects and the conservation of angular momentum. In simpler terms, a massive spinning object, in an effort to maintain its angular momentum, will provide forces opposing those which make the bicycle unstable. As long as the object has enough mass and rotates at a high enough speed, the forces are enough to prevent tipping over. Within this category, two different orientations are most common. Recall that the angular momentum vector of a spinning object is parallel to the axis about which it spins. In Fig. **??**, a spinning top has its angular momentum vector either pointing straight up or straight down, depending on if it spins clockwise or counterclockwise. Additionally, a spinning wheel, shown in Fig. **??**, of a bicycle has its angular momentum vector pointing perpendicularly out from the bicycle. The spinning top and wheel orientations are most common for the gyroscope. As one can see, in order for the gyroscope to be effective, the angular momentum vector must be perpendicular to the direction of motion. In the following sections, we will give an overview of each gyroscopic bicycle that we have been able to find in existence.

1.2.1 Bicycle Robot

Shown in Fig. 1.3, this bicycle uses a large gyroscope in a top orientation attached above the rear wheel to balance. It was built by Bui Trung Thanh at the Asian Institute of Technology. It is remote controlled and can balance while motionless, as well as in motion. There are motors on the front wheel to control steering direction and the back wheel to drive the bicycle. The robot was programmed using C on the ATMEGA128 micro-controller.

[2]Pyotr Shilovsky. Shilovski Gyrocar. Digital image. Wikipedia. Web. 30 October 2015.

Figure 1.3: Bicycle Robot.[3]

1.2.2 JyroBike

The JyroBike is one of the only commercially-available self-stabilizing bicycles. The bicycle is shown in Fig. 1.4. It balances by using a flywheel, which is simply a gyroscope in its wheel orientation. The flywheel is placed inside the front wheel and spins separately from the wheel itself. The JyroBike product is available as both the entire bicycle or the standalone front wheel with the flywheel. As a commercial product, it includes many features not found in other gyroscopic bicycles, such as a power button, flywheel speed control, and a rechargeable battery.

[3]Bui Trung Thanh. Bicycle Robot. Digital image. Youtube. Web. 30 October 2015.

Figure 1.4: JyroBike.[4]

1.2.3 2012 BicyRobo Thailand Competition Runner-Up

A team from King Mongkut's University of Technology created a self-balancing robotic bicycle using gyroscopes. This bicycle was created to compete in the 2012 BicyRobo Thailand Competition, which is a competition for self-stabilizing bicycles hosted by the Asian Institute of Technology in Thailand. It uses two gyroscopes in the top orientation, one on either side of the bicycle. As the bicycle tips to one side, the platforms that the gyroscopes are placed on tip forwards and backwards to balance the bicycle. This entails the use of sensors to detect tilt, such as an IMU or an accelerometer.

1.2.4 Lit Motors

Lit Motors is another company that seeks to commercially market their self-stabilizing vehicle. Their main product, the C-1, is a fully electric two-wheeled self-balancing motorcycle. As you can see in Fig. 1.7, the vehicle has doors, headlights, brake lights, and windows like a car, but has only two wheels. The C-1 is still in development, but some basic information about its design is available online. It balances using two

[4]JyroBike LTD. JyroBike. Digital image. KickStarter. Web. 30 October 2015.

gyroscopes and is powered by lithium iron phosphate batteries. The gyroscopes enable the motorcycle to lean in and out of turns, as a non-stabilizing motorcycle would. It weighs 800 lbs and can ride up to 200 miles on one charge. By comparison, most electric motorcycles weigh downwards of 500 lbs and can ride up to similar distances on a single charge.

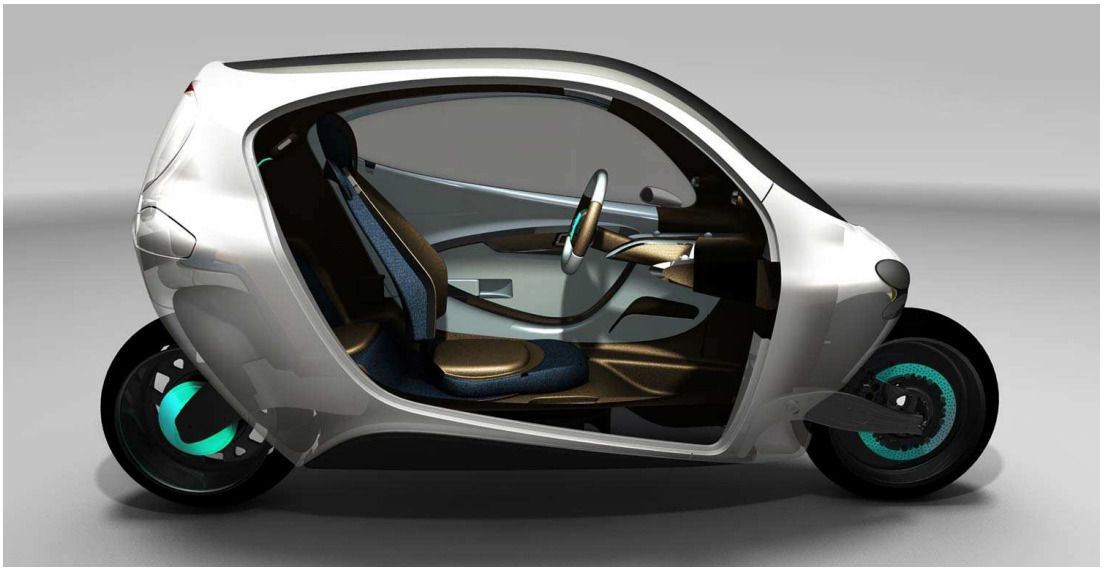

Figure 1.5: C-1 electric motorcycle by Lit Motors.[5]

1.2.5 Why Don't We Use Gyroscopes?

Although gyroscopes are highly stable, the use of a gyroscope requires a very complicated design with high weight and cost. This is because the wheel needs to be massive enough and needs to be spinning continuously in order for the bicycle to remain stable. This entails an incredible drain in energy and is not sustainable. As mentioned above, the weight ratio between the C-1 electric balancing motorcycle and regular electric motorcycles is close to 1.6. Additionally, a gyroscope often resists turns as a consequence of its high stability. Riding a gyroscopic bicycle is analogous to riding a tricycle. A tricycle, as we all know, provides stability to a bicycle with the addition of training wheels on either side. However, this provides too much stability since the rider is unable to lean into a turn as he or she would on a regular bicycle. The two training wheels prevent any tilt in the bicycles motion; to turn, the rider is forced to lean in the opposite direction. Gyroscopic bicycles are similar in that they are counterproductive in both teaching how to ride a bicycle and learning how humans balance on bicycles.

[5]Lit Motors. C-1 Electric Motorcycle. Digital image. Lit Motors. Web. 30 October 2015.

1.3 Balance by Reaction Wheel

The reaction wheel category consists of bicycles that again use a massive wheel with a high moment of inertia. However, instead of having a continuously spinning wheel, the reaction wheel only spins when necessary, to provide sufficient torque to counteract gravity and keep the bicycle from falling. This is also possible through the conservation of angular momentum; as the reaction wheel spins in one direction, it applies a torque on the bicycle in the opposite direction. Since the amount of torque is proportional to how fast the reaction wheel spins, it can be calculated very precisely to keep the bicycle very stable. The reaction wheel also differs from a gyroscope in that it is generally placed perpendicular to the axis of the bike and the ground, similar to the orientation of a steering wheel. Of the reaction-wheel-balanced bicycles found in research, none exhibited the ability to turn. Most either follow a straight path or only stay upright. Although the reaction wheel is also a very stable method, it is not suitable for our purposes, as shown in the following sections.

1.3.1 Auto Balanced Robotic Bicycle (ABRB)

Students at George Mason University built a two-inline-wheel robot capable of self-balancing using a reaction wheel. See Fig. **??** for a detailed schematic and Fig. **??** for the completed product. The design is fairly simple: a low-riding scooter with fixed wheels. The wheels were 12-inch bicycle wheels and the reaction wheel was placed roughly in the middle of the robot with a diameter of 8 inches. In order to attain a high moment of inertia while limiting the overall mass, the reaction wheel was custom machined out of steel to have its mass concentrated on the outer edge. The ABRB has been tested to perform well when driving forwards, backwards, and stopping. It also performed well under conditions when small disturbances were introduced.
The ABRB balancing system used a Motorola M68HC11 microcontroller and two sensors to read tilt angle: the ADIS16209 inclinometer and the ADXRS401 gyroscope. The redundancy in these devices was used to correct for gyrscopic drift. The ABRB drive system used two different microcontrollers: the AVR ATmega32 from Atmel and an AVR ATtiny25 also from Atmel. The first was used for the more complex drive control logic and the latter was used to receive signals from a hand-held remote control. The drive motor used was a Pittman 8712 brushed DC motor.

Figure 1.6: ABRB completed design.[6]

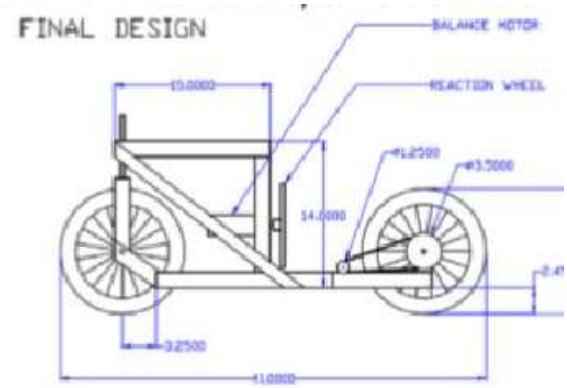

Figure 1.7: ABRB schematic design.[7]

1.3.2 One Track Vehicle

A researcher by the name of Gunnar Schmidt created a similar robot at the Technical University of Berlin. He started his design incrementally by first building a robot to balance an inverted pendulum with small disturbances using the CHR-6DOF IMU to detect tilt angles. The final reaction wheel used was a 12 inch bicycle wheel with metal plates around its edge to give it a larger moment of inertia. Unlike above, this bicycle was only tested to maintain balance while motionless. The final specifications were 25.2 kg for the bicycle with 7.4 kg attributed to the reaction wheel. The motor used was a Faulhaber DC motor. This bicycle was less of a success than that of above, since it was seen to exhibit oscillations under certain condiditons, which can be attributed to flaws in the controller feedback loop. The bicycle can be found below in Fig. **??**.

[6]George Mason University. Auto Balanced Robotic Bicycle. Digital image. George Mason University. Web. 30 October 2015.

[7]George Mason University. Auto Balanced Robotic Bicycle. Digital image. George Mason University. Web. 30 October 2015.

Figure 1.8: One Track Vehicle.[8]

1.3.3 Why Don't we Use Reaction Wheels

Reaction wheels exhibit the same major flaw as gyroscopes: they must be heavy enough! This limits the weight for other components on the vehicle since a bicycle is largely thought to be light enough to carry, if needed. Additionally, both bicycles shown above have no means of turning. That is not to say that turning would be impossible to accomplish with a reaction-wheel-balanced bicycle, it just has not been done yet. Additionally, imagine how difficult it would be to ride a bicycle that would jerk upright every time it began to tilt. For the interest of studying human balance on bicycles and the goal of completing a safer, ride-able, learning bicycle, the reaction wheel design entails many characteristics that are ultimately unhelpful.

1.4 Balance by Steering

The last category is the one our team is interested in: balance by steering. This category consists of bicycles that simply steer to correct tilt angle and keep the bicycle stable. This method is most akin to how humans generally ride bicycles and is most suitable for our goals. The method itself does not entail many design constraints other than an extra motor to control steering, which is akin to the extra motor for the two categories

[8]Gunnar Schmidt. One Track Vehicle. Digital image. Technical University of Berlin. Web. 30 October 2015.

previously. However, with balance by steering unlike the previous category, there is no longer the weight constraint. Despite this apparent advantage, a common trend appeared amongst bicycles that use steering to balance. Bicycles that used steering for balance were either highly unstable or were only stable at moderately high speeds. These bicycles were seen to be very wobbly, even when undisturbed.

1.4.1 RoboRealm Robotic Bicycle

The Science and Technology Research Institute (STRI) Robotics Team built an auto-balanced, auto-steering, ride-able robotic bicycle, shown in Fig. 1.9 to enter in the BicycRobo Thailand Competition in 2010. The bicycle can only balance while moving at moderately high speeds and is can be controlled either remotely or via image processing. It uses a combination of encoders, potentiometers, gyroscopes, and accelerometers for sensor data, as well as a webcam for image processing. It is only moderately stable, as it experiences slight jitters due to either over or under-compensation by the steering wheel.

Figure 1.9: RoboRealm Robotic Bicycle.[9]

1.4.2 Micro Robot Bicycle

The Micro Robot Team from the Mahanakorn University of Technology built a bicycle similar to the one above that balances by steering for the same competition. It uses a compass for navigation as well as some form of image processing. This bike, similar to the one above, also seems to have trouble riding in a straight line without veering off course. Additionally, it is unable to maintain stability at zero speed.

[9]STRI Robot Team. RoboRealm. Digital image. Science and Technology Research Institute. Web. 30 October 2015.

1.4.3 RoboBiker

This robot was built by Masahiko Yamaguchi and emulates how a human rides a bicycle. It consists of a human-like robot (about 6 inches high) sitting on a miniature bicycle pedaling with its feet and controlling steer with its hands, as shown in Fig. **??**. The robot uses a Tamagawa Seiki TAG201 gyro and a PID controller to calculate steer angle adjustments. It is also remote-controlled. The bicycle itself is a fixed-gear bicycle but has no brakes, so the robot must slam its feet down on the ground to stop movement. It also cannot balance while motionless and is rather wobbly.

Figure 1.10: RoboBiker.[10]

1.4.4 Self Stabilizing Electric Bicycle

Developed in Keio University, this electric bicycle can balance while in motion and is ride-able. It uses a gyroscopic sensor to detect changes in tilt while a camera tracks an LED mounted to the back to detect movement. The setup is shown in Fig. 1.11. Thus far, it has only been tested on rollers and only in straight lines. The controller it uses is sophisticated enough to vary and adjust both speed and steering if it happens to begin to fall. The final goal is to create a bicycle that will serve as a convenient alternative to a small car. The researchers at Keio University, Yasuhito Tanaka and

[10]Masahiko Yamaguchi. RoboBiker. Digital image. DesignBoom. Web. 30 October 2015.

Tohsiyuki Murakami, aim to be able to stabilize the bicycle at zero speed, implying that it does not yet exhibit the ability to do that.

Figure 1.11: Self Stabilizing Electric Bicycle.[11]

1.4.5 Ghostrider

Shown in Fig. 1.12, the Ghostrider was built to enter in the DARPA Grand Challenge by a team at the University of California, Berkeley. In building the robotic motorcycle, the team also built a custom Inertial Angle Sensor, capable of 100KHz baud rate and 0.02 degrees resolution. Despite this custom sensor, the motorcycle itself is very wobbly and cannot balance while motionless. It uses both GPS and image processing to navigate past obstacles.

Figure 1.12: Ghostrider.[12]

[11] Keio University. Self Stabilizing Electric Bicycle. Digital image. Phys.org. Web. 30 October 2015.

1.4.6 NXTBike-GS

Built at the Delft University of Technology, this robot, as seen in Fig. 1.13, was built out of Lego pieces and programmed using a Lego Mindstorms NXT. The robot also uses a rotary encoder for steering the front wheel and a Hitechnics Gyro Sensor to detect tilt. Another DC motor was used to drive the back wheel. Although the robot is small, it still exhibits some wobble in its path. Unlike its less successful counterparts, it is able to turn and balance while turning, though it cannot balance while motionless.

Figure 1.13: NXTBike-GS (Legos).[13]

1.5 Goals

As shown in the preceding sections, a steering bicycle with the ability to balance while motionless has yet to be built. Even amongst the bicycles/motorcycles already built that use balance by steering, none exhibit high stability and high recoverability. Our goals include building an autonomous bicycle that falls in the third category that not

[12]University of California at Berkeley. Ghostrider. Digital image. WeMakeMoneyNotArts. Web. 30 October 2015.

[13]Delft University of Technology. NXTBike-GS. Digital image. Mathworks. Web. 30 October 2015.

only is highly stable at low/zero speeds but can also easily recover from external disturbances. We also aim to have the bicycle navigationally autonomous, by using GPS and image processing. Very few existing bikes were found to have the ability to navigate autonomously and those that did, were not meant to leave a pre-designated track with clear lanes.

Chapter 2

Bicycle Dynamics and Development of a Controller for Stability and a State Observer

Contributors: Arundathi Sharma
This chapter is a synthesis of the Autonomous Bicycle Project's Fall 2014 and Spring 2015 Dynamics and Controls Paper, by Shihao Wang, Joong Gon Yim, Alex Abrams, and Binghan He

In this section, we present the mathematical model of the bicycle that we are using and derive the equations of motion for such a bicycle. We also review the derivation of a stabilizing controller that should keep the bicycle upright, and the development of an observer, which will estimate the state of the bicycle.

2.1 Dynamics: Deriving a Linearized Equation of Motion

2.1.1 Point Mass Model

[INCLUDE PICTURE OF DIAGRAM WITH LABELED ANGLES]
From the figure above, we define geometry as follows:

G = *center of mass*
$\overline{AD}$ =*front fork*
$\overline{BG}$=b
l = *wheelbase* $\overline{AB}$
ϕ = *lean angle*
ψ = *yaw angle (heading)*

δ = *steer angle*
α = *angle between front wheel and* $\overline{CD}$
x_G = *x-position of the center of mass*
y_G = *y-position of the center of mass*
z_G = *z-position of the center of mass*
v = *forward velocity of bicycle (assumed constant)*
C = *the contact point between the rear wheel and ground*
D = *the contact point between the front wheel and ground*

2.1.2 Deriving and Linearizing the Equation of Motion

We use the physical model of the bicycle outlined above to find an equation describing the motion of the bicycle's center of mass. Refer to Shihao Wang's Fall 2014 report in the appendix for a detailed kinematic derivation. The resultant equation is:

$$\begin{aligned}\vec{a}_G = (\dot{v} - h\cos(\phi)(\dot{\phi})\dot{\psi} - h\sin(\phi)\ddot{\psi} - h\cos(\phi)\dot{\phi}\dot{\psi} - b\dot{\phi}^2)\hat{\lambda} + \\ +(b\ddot{\psi} - h\sin(\phi)\ddot{\phi} + v\dot{\psi} - h\sin(\phi)\dot{\psi}^2)\hat{n} - (h\cos(\phi)\dot{\phi}^2 + h\sin(\phi)\ddot{\phi})\hat{k}\end{aligned} \tag{2.1}$$

where $\hat{\lambda}$ runs parallel to the bicycle's direction of motion, $\hat{n}$ is normal to $\hat{\lambda}$ in the ground plane, and $\hat{k}$ points opposite to earth's gravity.
This equation is useful, but we want to use this equation to control a bicycle. What parameters are out of our control? We cannot control $\dot{\psi}$, $\ddot{\psi}$, and α. Note: α is distinct from δ because for a given steer angle, the angle α changes as the bicycle leans.

Again, see the appendix for a fully detailed derivation, the results of which are:

$$\dot{\psi} = \frac{v\tan\alpha}{l}$$

and

$$\tan\alpha = \frac{\tan\delta}{\cos\phi}$$

Putting these two expressions together, and then taking a derivative to obtain $\ddot{\psi}$, we can substitute into the original equation to describe the acceleration of the bicycle's center of mass using only lean and steer angle terms. We can measure lean and steer angles, and can control steer angle, so this equation is what we want.

Now, we use our information about the motion of the center of mass to obtain a differential equation. (See appendix for full derivation). This is done by performing

an angular momentum balance about point C (rear wheel contact point with ground). Taking forward velocity v to be constant, we obtain an equation that contains the most important parameters: lean angle, angular velocity, and acceleration, and steer angle and angular velocity. Since we want to work with a first-order linear differential equation, we linearize the equation that we just found by using standard small-angle approximations for $\sin\theta$, $\tan\theta$, and $\cos\theta$. Although the bicycle is a nonlinear system (which we see in our non-linear equation of motion), we approximate its motion in a small region about the desired equilibrium point ($\phi = 0$, for straight riding) as linear. Note that if we deviate too much from a particular small region about equilibrium, our controller may not be able to recover from a perturbation because the bicycle's behavior will no longer be linear. Eventually, (see appendix for algebra) we obtain a linearized expression that looks like:

$$v^2\delta + bv\dot{\delta} = hl\ddot{\phi} - gl\phi$$

. Rearranging for the relevant term:

$$\ddot{\phi} = \frac{g}{h}\phi - \frac{v^2}{hl}\delta - \frac{bv}{hl}\dot{\delta}$$

2.2 Developing a Controller

From the above differential form, we can put our equation into state space form, which is a useful form for developing a controller. It looks like:

$$\begin{bmatrix}\dot{\phi}\\ \ddot{\phi}\\ \dot{\delta}\end{bmatrix} = \begin{bmatrix}0 & 1 & 0\\ \frac{g}{h} & 0 & -\frac{v^2}{hl}\\ 0 & 0 & 0\end{bmatrix}\begin{bmatrix}\phi\\ \dot{\phi}\\ \delta\end{bmatrix} + \begin{bmatrix}0\\ -\frac{bv}{hl}\\ 1\end{bmatrix}\dot{\delta}$$

Observe that if we evaluate the right-hand side of the above equation, we will obtain a set of three differential equations that apply to our system. We call $x = \begin{bmatrix}\phi\\ \dot{\phi}\\ \delta\end{bmatrix}$ our state, which fully defines our system, the bicycle. If we know these three parameters, we have fully defined the state of the bicycle at a moment in time. In a general sense, the equation above is the same as:

$$\dot{x} = Ax + Bu,$$

where the matrices A and B are properties of our system. A describes the extent to which the state of the system is affected by itself i.e., how do the values of $\phi, \dot{\phi}, \delta$ at a point in time affect how those values change in time ($\dot{\phi}, \ddot{\phi}, \dot{\delta}$). You might also call this

the natural behavior of the system. The eigenvalues of A would give us the solution to the differential equations that we used to produce this state space equation. B describes the extent to which our control input signal, $u = -Kx$ ($\dot{\delta}$ for the bicycle), affects the state. We want to develop a controller, represented by a matrix K, such that the above generalized equation can be rewritten as:

$$\dot{x} = (A - BK)x,$$

We also define an output $y = Cx$, which represents our control variable:

$$y = \begin{bmatrix} 1 & 0 & 0 \end{bmatrix} \begin{bmatrix} \phi \\ \dot{\phi} \\ \delta \end{bmatrix}$$

As you can see, it outputs a value ϕ. Ideally, we want our input and output to eventually be equal values.

To design the controller, we need to consider some A_{des}, which represents the desired behavior of the system, as it is affected by its own, controlled state (analogous to A in $\dot{x} = Ax + Bu$. Just as the eigenvalues of matrix A would describe the solutions to the differential equation that we used to derive the *original* behavior of the system, the eigenvalues of A_{des} represent the solutions to the differential equation describing our *desired* behavior. So we use this fact to solve for a suitable K.

2.2.1 Controller for Stability

We find K according to our design requirements for the controlled behavior of the bicycle. In our case, we want the bicycle to stabilize itself in a short amount of time, say under 0.1s. We also want to prevent the bicycle from oscillating about $\phi = 0$ at high frequency. To do this, we assign a desired overshoot to our control response to be less than 5%. <-CHECK THIS
We can employ a number of different methods to actually develop a controller that meets these requirements. You can see what these methods are and how they were employed to obtain a controller in the appendix section. The important thing is that we went on to develop such a controller for a point-mass bicycle stabilization:

$$K = \begin{bmatrix} -843.1298 & -119.7419 & 8.2379 \end{bmatrix}$$

When this was put into a basic MATLAB simulation, these were the plots we obtained, to describe the behavior of the bicycle.

[INSERT PICTURES OF PLOTS FROM SHIHAO'S REPORT]
Based on these plots, the theoretical bicycle stabilizes within the desired time frame from a initial displacement lean angle $\phi = \frac{\pi}{4}$. Furthermore, the bicycle trajectory behaves as we expect it to for this situation, so this controller can, at least in theory, successfully balance a bicycle modeled as a point-mass.

What of the actual bicycle? The controller above was derived using guessed values for certain parts of the bicycle geometry. But since we are trying to develop a controller for our own bicycle, we can customize. We can pretend the real bicycle is a point-mass by finding its center of mass, and then plugging in relevant parameters in order to find a controller that will work specifically for our bicycle. Quoting the Spring 2015 Controls report:

"In order to design a controller for the bicycle, we should know the value of the geometric parameters of the real bicycle. Mass doesn't appear in the A or B matrices, and g is a constant. Therefore, we only need to measure the position of the center of mass (COM) relative to the rear wheel contact point C. We can find the center of mass of an irregular object quite easily. If we let it hang freely, the center of mass is directly below where we hang it from. If we then hang the object from a couple of other points and draw the lines that go vertically downwards, the center of mass is where the lines meet."

INSERT PICTURE OF BICYCLE
Here are the parameters that were measured off the real bicycle:

- $l = 0.9144m$, wheel base distance
- $b = 0.331m$, horizontal distance between COM and rear wheel contact point
- $d = 0.5834$
- $h = 0.3445m$, height of COM
- $v = 3.57m/s$, forward speed
- $g = 9.81\frac{m}{s^2}$, gravity constant

Now, using these values for the real bicycle and implementing them in the same way as we did before, we obtain a new, perhaps more applicable controller than the one where we assumed arbitrary values for those numbers:

$$K = \begin{bmatrix} -3.4215 & -0.8439 & 4.3345 \end{bmatrix}$$

With an initial lean of $\pi/6$, this controller also appears to stabilize a bicycle in a simple MATLAB ode45 simulation:

INSERT PLOTS
The three big problems that we could encounter with this controller are:

- Since the real bicycle is a nonlinear system, the nonlinear terms in the equation of motion will dominate its motion when our linearization approximation becomes invalid outside a certain range
- The controller may or may not be able to account for inaccuracies in the measured or calculated parameters for the bicycle
- The method used to construct this controller is subjective (see: pole placement method)
- Our control variable is $\dot{\delta}$. Ideally, we want to make the most out of the output torque from our steering motor, so we should design our controller such that the maximum steer angular velocity required to turn the handlebars at any time would be 400rpm (the rating for our 24V 80W Maxon F 2260 motor).

So, we can work off our initial controller to optimize it further and ensure it is robust enough to balance our bicycle. This is done by an algorithm called Linear-quadratic Regulator (LQR), which is a more systematic way of finding a controller. This makes it suitable for automation. MATLAB has a command that performs this optimization, and gives us the following:

$$K = \begin{bmatrix} -38.3748 & -4.1949 & 9.5922 \end{bmatrix}$$

Again, we perform a simulation, and from an initial lean angle $\phi = \frac{\pi}{3}$ and obtain the following plots, showing that the bike stabilizes:
INSERT PLOTS

2.2.2 Observer-based Controller for Reference Tracking

We developed the controller in the previous subsection under the assumption that we knew all the state variables. However, in real life, that may not be the case. So, we create an observer-based controller. A state observer will estimate our state variables based on measurements that we make of the control variable (lean angle, in our case) and other output variables. The observer has the same mathematical form as the system itself, because it is trying to estimate the state. Meanwhile, the controller is trying to achieve the desired state (whatever that may be–it may be different from $\phi = 0$ in case we have a different reference trajectory, e.g., when the bicycle is turning). The observer looks like:

$$\dot{\hat{x}} = A\hat{x} + Bu + H(y - C\hat{x}),$$

where $u = -K\hat{x}$, $\hat{x}$ is our estimate of the state, y is the output, and x is the actual state. We are interested in the accuracy of our estimate, so we define an error, $e = x - \tilde{x}$, so that our equation above can be more usefully expressed as:

$$\dot{e} = (A - HC)e$$

Just as we previously wanted some matrix A_{des} such that the bicycle would behave a certain way, we want to find $A - HC$ such that the observer behaves a certain way; specifically, we want our error, e, to become zero as quickly as possible. Again, we can find a matrix H that makes this possible, just as we found K previously. The methods for doing this are very similar to those used to find the stability controller, and are detailed in the appendix. What we ultimately come up with is a value for H as follows:

$$H = \begin{bmatrix} 78 \\ 2028 \\ -11137 \end{bmatrix}$$

Putting the assembled controller with observer, we hope to see how our controller's step response. In MATLAB, this is what we see:
INCLUDE PLOT
This shows good behavior (convergence to 1), and a rise time under 0.1s, making the controller suitable for our purposes, at least as a starting point.

It is important to point out that we actually have access to all of our state variables, so it may not appear that the state observer is actually necessary. However, this will become more useful in the future, when we may implement GPS control. If we are trying to find our universal position (Earth's reference frame), we will need to know our yaw and yaw angular velocity ($\psi, \dot{\psi}$). In that situation, the state observer will become more useful, as we try to have the bicycle navigate a closed course.

2.3 References

References to published work should be given consistently in a format that is currently accepted in the field of work covered by the thesis. If in doubt, candidates should consult their supervisors about the best method.

2.4 Binding and lettering

Theses may be presented for examination in either permanent or temporary bindings.

Permanent binding The thesis to be bound in book form in a strong cloth of any suitable colour. Maximum thickness 65 mm (2.5"): if of greater thickness, two or more volumes per copy will be required. The binding of all volumes must be identical. The thesis should be bound in such a way that it can be opened fully for ease of microfilming. Final hardbinding is undertaken off university campus by SRJ Ltd in Liverpool (phone: 0151 709 1354). Visit their website: http://www.srjservices.co.uk/. Lettering on permanent bindings to be in gold. Front cover: title of thesis. Spine: Top: degree. Middle: surname and initials. Bottom: year of submission.

Temporary binding The thesis should be presented in such a way that the pages cannot be readily removed. The use of ring binders is therefore not permitted. The candidate's surname, initials, the date (month and year) and the degree to be shown on the outside front cover. Softbinding of initial submission can be undertaken by the university print unit. After the thesis has been approved by the Examiners, two copies must be permanently bound as above and deposited with the Dean of the candidate's Faculty before arrangements for the conferment of the degree can be made.

2.5 Abstract

Each copy of the thesis must be accompanied by a separate copy of the Abstract indicating the aims of the investigation and the results achieved. For microfilming purposes it must:

- Be typed or printed although good photocopies are acceptable;
- be not longer than can be accomplished by single-spaced type on one side of an A4 sheet (about 450 words);
- show the author and title of the thesis in the form of a heading.

2.6 Paper

A4 white bond paper of 70 to 100 g/m^2 weight must be used for both originals and photocopies, except for any endpapers which carry no text. If both sides of the paper are used for text, then:

- Both sides must be used in both copies which are to be permanently bound;
- there must be little or no 'show-through' - paper lighter than 80 g/m^2 should not be used;

- the full binding margin of 40 mm must be allowed on the left side of odd pages and the right side of even pages - other margins must be 25mm minimum.

Margins and line spacing $1\frac{1}{2}$ spacing is advised, but at least double line spacing should be used for text that contains many subscripts and superscripts. Quotations may be indented. Authors should check the text carefully for 'widows and orphans' and make full use of all error-checking facilities.

2.7 Page numbers

Pages should be numbered consecutively and the position of page numbers (candidate's choice or as advised by the supervisor) should be consistent throughout.

2.8 Footnotes

Footnotes should be inserted at the foot of the relevant page in single line spacing. Smaller type may be used, if available. A line should be ruled between footnotes and the text. Footnotes should be numbered consecutively throughout the thesis.

2.9 Further advice

The following publications, which can be consulted in the University Libraries, give advice on the preparation of theses and methods of bibliographical reference. Students are advised to purchase their own copies of their chosen manual.

2.9.1 For Humanities and Social Sciences

MHRA Style Book, Modern Humanities Research Association, London. MLA Style Sheet, Modern Language Association of America, Baltimore.

Watson, G: *Writing a thesis: A guide to long essays and dissertations.* Longman, 1987. Turabian, K L: A manual for writers of term papers, theses and dissertations. University of Chicago Press, Chicago, 1987.

2.9.2 For Sciences, Engineering and Medicine

Barrass, R: *Scientists must write: A guide to better writing for scientists, engineers and students.* Science Paperbacks, Chapman & Hall, 1978.

Booth, V: Communicating in science: *Writing and speaking.* Cambridge University Press.

Lindsay, D: *Guide to scientific writing — a manual for students and research workers.* Longman, London, 1990.

Lock, S: *Thorne's better medical writing.* Pitman, London, 1977. O'Connor, M and Woodford, F P: *Writing scientific papers in English: An Else-Ciba Foundation guide for authors.* Elsevier, Amsterdam, 1976.

2.9.3 For all candidates

Stanisstreet, M: *Writing your thesis: Suggestions for planning and writing theses and dissertations in science-based disciplines.* University of Liverpool Research Sub-Committee, 1988.

Stanisstreet, M: *Preparing for your viva: Suggestions for preparing for postgraduate vivas in science-based disciplines.* University of Liverpool Research Sub-Committee, 1988.

These booklets were written by a scientist with scientists principally in mind, but much of the advice therein will benefit those in other disciplines. Copies are normally issued automatically to research students in science- based departments. They may also be obtained on request, free of charge, from Faculty Offices and the Student & Examinations Division, Senate House.

Chapter 3

Inertial Measurement Unit

Contributors: Jason Hwang & Sung Won An

3.1 Background

The focus of this chapter will be on the Inertial Measurement Unit (IMU). IMUs are orientation sensors which use a combination of gyroscopes and accelerometers to provide information regarding the sensor's position and angular rates.

The specific IMU used for the autonomous bike is the Microstrain Inertia-Link. The purpose of using an IMU for the bike is to provide information regarding the bike's roll angle and angular roll rate. The roll angle tells us how much the bike is leaning to its side, and the angular roll rate tells us how quickly it is falling. Using the two values will allow the control system to correct the bike's lean position so that it balances.

3.1.1 Six Degrees of Freedom

The IMU is capable of reading its position in three dimensional space by using six sensors. Each of the sensors within corresponds to a certain direction of motion; there are three sensors for the XYZ directions and three sensors for the roll, pitch, and yaw directions. The IMU uses a triaxial accelerometer to determine the changes in acceleration in the XYZ direction and gyroscopes to measure roll, pitch, and yaw.

A tiny object of known mass lies in each sensor and the acceleration is found by determining how much the object moves. Similarly, the IMU uses the triaxial angular rate gyros to determine how the IMU moves in the roll, pitch, and yaw directions. From the sensors, the IMU can predict how the IMU is positioned in regards to the roll, pitch and yaw angles (further details are described below).

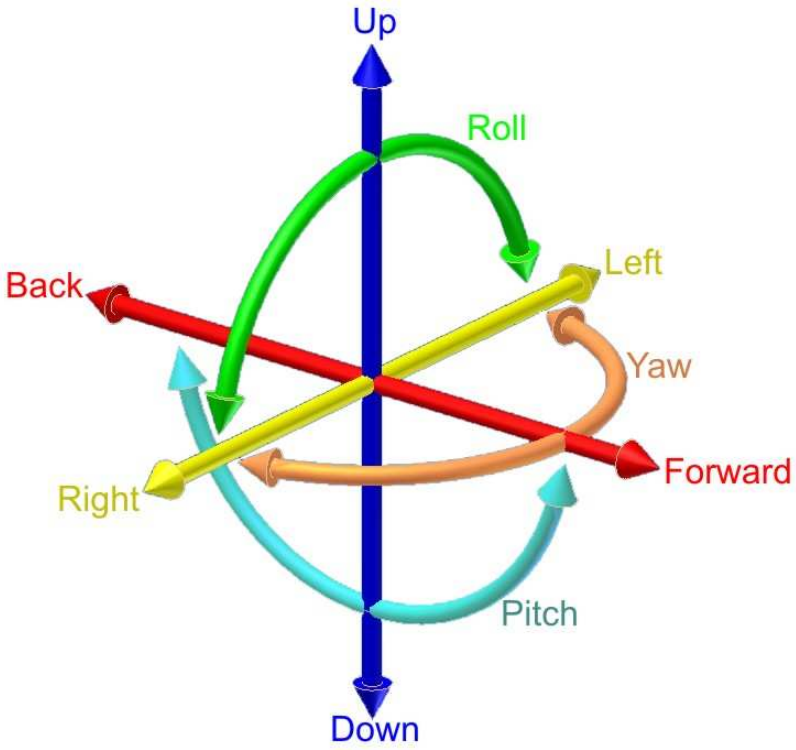

Figure 3.1: Six Degrees of Freedom[1]

3.1.2 Euler Angles and Angular Rates

The roll, pitch, and yaw directions are also known as Euler angles. The IMU derives the Euler angles in radians from a 3x3 rotation matrix. The elements in the 3x3 rotation matrix describe the relation between the Earth's fixed coordinate system and the IMU's own local coordinate system. Thus, the IMU determines its position by comparing its own location relative to the fixed Earth coordinate system.

The angular rates describe how fast the Euler angles are changing with respect to time. These values are determined directly from the angular rate gyro sensors.

The Euler angles which describe the position of the IMU are mathematically obtained by integrating the angular rates, after conversion to the proper coordinate frame is done. One property of Euler angles is that the pitch is incorrect when the pitch is greater than $\pm 90°$. This issue isn't relevant to the bike as the bike would always be flat on the ground.

[1] https://en.wikipedia.org/wiki/Six_degrees_of_freedom/media/File:6DOF_en.jpg

3.1.3 Drift

One disadvantage of IMUs is that they accumulate error over time. As all IMUs have a certain amount of noise, they tend to drift in accuracy over time. Each new value (which contains noise) is added to previously found values (which also contain noise) and all traces of past errors becomes accumulated. The amount of noise specified for the Inertia-Link Microstrain IMU is $\pm 0.5^\circ$ when still and $\pm 2.0^\circ$ when in motion. However, noise was determined to be small enough to be insignificant as concluded from tests detailed in later sections.

3.1.4 GyroBias Correction

GyroBias correction can be used to compensate for any bias errors in the angular rate gyros in terms of the x, y, and z components. Each XYZ value corresponds to an angular rate sensor: X-Roll, Y-Pitch, Z-Yaw. For example, the roll is determined when the IMU is rotated about the x-axis when all other angles are fixed. The GyroBias values are stored in a vector with units $\frac{rad}{sec}$ and each value is applied to all subsequent values in the angular rate vector. The GyroBias is in terms of the IMU's local coordinate system. Upon start up, the GyroBias vector is initially $[0, 0, 0]$.

3.2 Code

All programs for the IMU are written in Python, since Python is used on the BeagleBone Black. Using the same programming language allows the IMU to work seamlessly with the other bike components.

3.2.1 Testing

Testing was done to determine the accuracy and reliability of the IMU. Tests were done through a computer-to-IMU connection to allow quicker debugging and easier data collection. The primary focus of the tests were geared towards determining the accuracy of the roll angle. This is because it is easier to determine the accuracy of the roll angle than the roll angular rate. Since the Euler angles and angular rates correlate to each other, theoretically if one is accurate, so is the other.

3.2.2 BeagleBone Black Code

There is a single module for interaction with the IMU, deservedly named imu.py. Within this module, there are 5 functions. The first two, bit_check() and imu_convert(), are

used to read data from the IMU. Bit_check() takes in a string of bytes read from the IMU and converts them into a byte representation that Python recognizes. The precondition for the input parameter is that it must be a string representing a hexadecimal number. The imu_convert() function converts a hexadecimal number into a floating point number and is often called immediately following the call to bit_check(). It takes in a parameter in the Python representation of hexadecimal numbers, which is why bit_check() must first be called to convert the data into the Python representation.
The next function is a parametrized valid_checksum() function that takes in raw data read from the IMU, the length of the data, and the original command written to the IMU. The IMU works as a poll and response device. When the user or system wants data from the IMU, a command byte must first be sent to the IMU so it knows what type of data to return. The valid_checksum() function adheres to the Data Communications Protocol used by the IMU and is used to ensure that the data received has not been corrupted in any way. The checksum works by summing together all but the last two bytes in the return message and comparing it against the last two bytes. If the two numbers match, then the checksum is valid. An issue that was discovered during testing was that there can often be an overflow issue with summing together multiple bytes is succession. To account for this, the sum modulo 65536 is used for comparison. The number 65536 represents the upper bound of an int in Python, before overflow occurs.

The last two functions are used to interact with the IMU. These functions, get_roll_angle_ang_rate() and correct_bias(), are used to retrieve the current state of the IMU and correct the gyroscopic bias of the IMU, respectively. The get_roll_angle_ang_rate() is a misnomer, since the command written to the IMU asks for not just the roll angle but pitch and yaw as well as all three angular rates. However, since the only value we are interested in is the roll angle and its rate of change, it only returns those two. The function prompts the IMU to return its current state, waits until all response bytes are ready, verifies the checksum, and returns the corresponding values. If the checksum is invalid, the function continues looping until it finds uncorrupted data. This may prove to be an issue in the future, since the microcontroller can stall in this function if the IMU becomes damaged.

The correct_bias() function prompts the IMU to run its internal Gyro Bias Correction protocol. The IMU can be prompted to run this protocol for anywhere between 10 and 30 seconds, with the latter resulting in a more accurate correction. During this time the IMU must remain completely still, but can be in any orientation. Otherwise, the Gyro Bias Correction may not be as effective. As this function was meant to be run upon startup, it is currently set to run for 30 seconds each iteration and loops until

the roll angle read is less than 0.5 degrees, which is the precision the IMU is rated for while motionless. Additionally, this assumes that the IMU is both completely still and parallel to the ground at 0 degrees. Since it is cumbersome to have to delay for 30 seconds during each startup, progress is being made to hard-code a Gyro Bias Correction matrix by taking an average over many calls to the function under a variety of situations and environments.

3.2.3 IMU to PC

While testing, it may be cumbersome to have to use the BeagleBone Black to communicate with the IMU, especially since we only have one microcontroller for the whole project. Instead, there is a module developed by former members of the Autonomous Bicycle Team that can interface directly to the IMU from any personal computer. This module was developed because the software that came with the IMU only runs on Windows and it doesn't allow the user to save data read from the IMU. This module, named RollAngle.py, takes advantage of the IMU USB connector and interacts with it serially. It uses UART to output values to the user and maintains much of the same functionality as found in the imu.py module. However, since we no longer have an intermediate microcontroller to buffer data through, the module implements its own Queue and Packet data structures. These data structures help maintain a circular buffer that continuously refreshes and overwrites old and useless data as more streams in. Using this module, we were able to read the state of the IMU and thanks to progress we've made this semester, we are now able to correct gyro bias as well. In addition, there is another version of this module that can plot values read from the IMU to a graph that we can store. This version was used to generate the plots from the multiple tests that were run on the IMU.

3.3 Results

The results from testing mainly addressed the accuracy and reliability of the IMU. From the collected results, we were able to determine what problems the IMU were encountering and how to address the issues. After implementing potential solutions, we would retest the IMU and observe if it provided more accurate data.

3.3.1 Without GyroBias

The initial tests were done without implementing GyroBias correction since not much about the IMU was understood at the time. The main goals were to see if the IMU

still worked from previous semesters and whether it was accurate enough for the bike. Different testing procedures were performed to examine how the IMU performed under different scenarios.

Flat-Roll-Flat

The purpose of the flat-roll-flat tests was to see how well the IMU performed when it was in motion and how it responded when returning to a specific angle. The initial position was chosen to be when the IMU laid flat on the table since that's when the roll angle should always be 0°. The accuracy of the IMU can then be determined by comparing the IMU's reported angle with the true angle of 0°.

The test was performed by first laying the IMU flat, rolling it in both the positive and negative directions, then laying it flat on the table again. The roll speed (ie. roll rate) was varied to see how the IMU performed under extreme (and at times unrealistic) conditions.

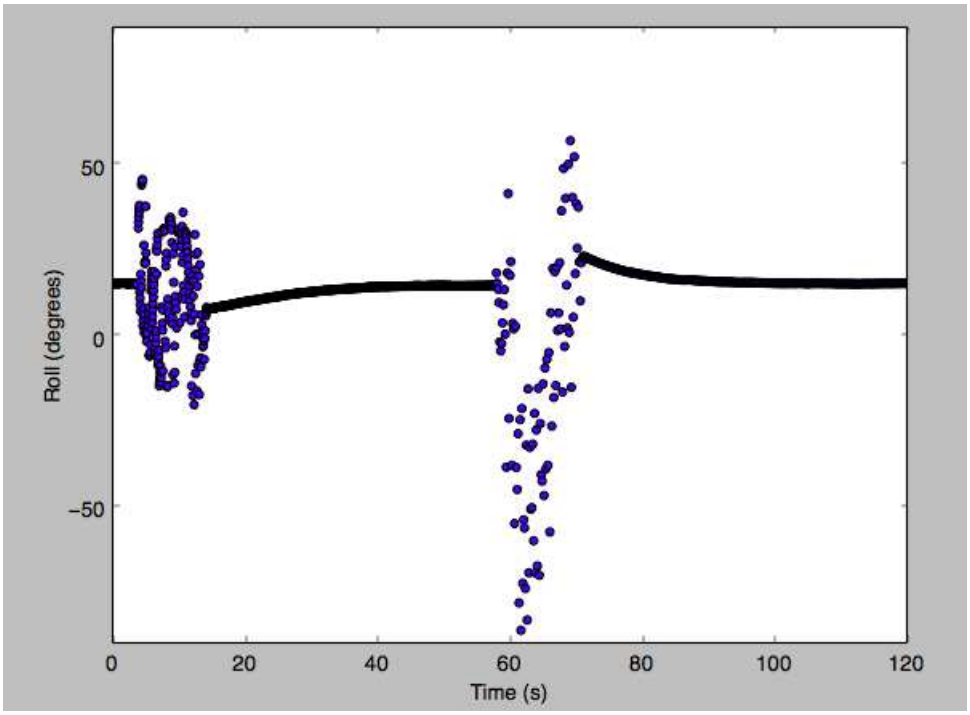

Figure 3.2: Flat-Roll-Flat:Fast

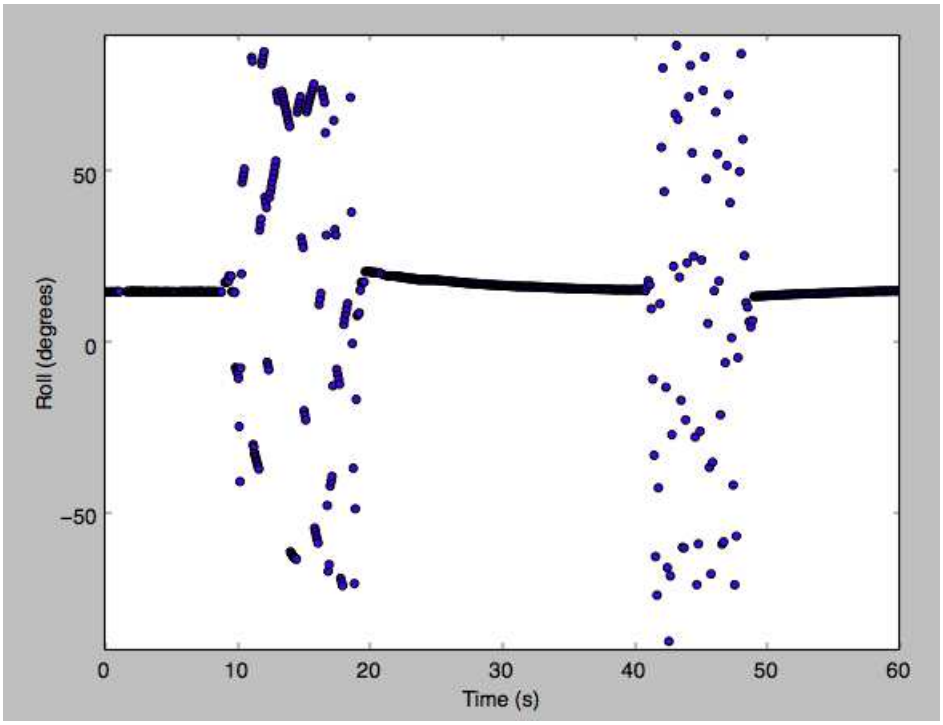

Figure 3.3: Flat-Roll-Flat:Medium

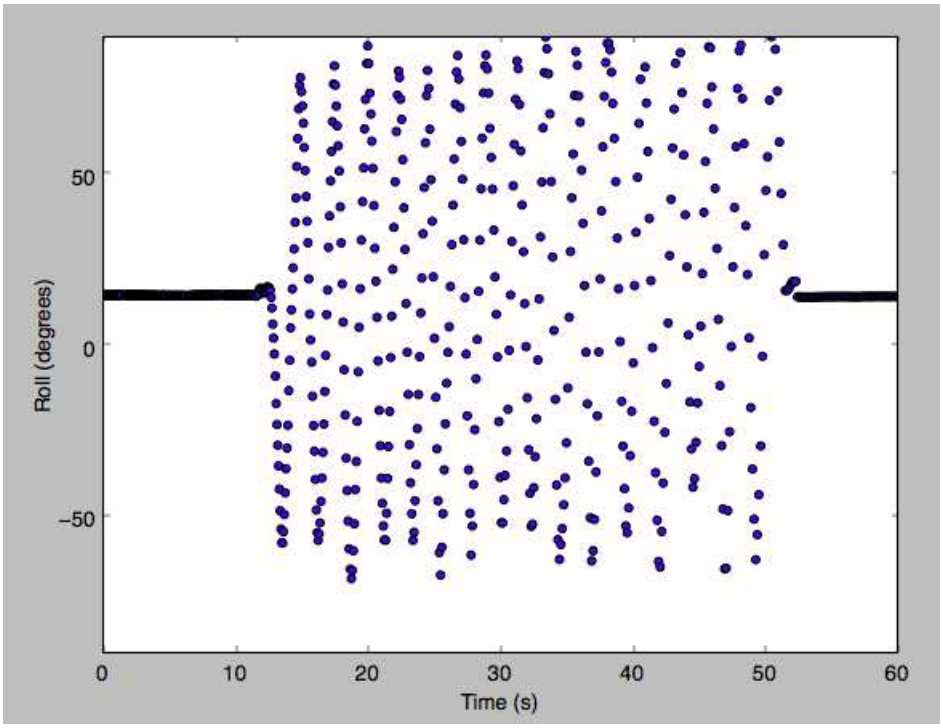

Figure 3.4: Flat-Roll-Flat:Slow

Observations

1. **The roll angle is offset by** 14°**.** When the IMU is flat, it should ideally read a

value of 0° yet it reads 14° and all subsequent readings are offset by that value. However, the roll angles reflect the ideal readings and are positive when the IMU is rolled to the positive direction and negative when rolled to the negative direction. The offset issue was addressed later on when performing a yaw vs roll test.

2. **IMU is most accurate when rotated at a slower pace.** When the IMU is rotated too quickly about the roll direction, the IMU is off by 7° after being placed back (flat position) when compared to its original starting angle of 14°. The IMU then takes 20 seconds to return back to its original reading. In terms of the bike, 20 seconds is too long for the bike to wait for an accurate reading.
When rotated at a slower pace, the IMU is accurate throughout the entire test. The roll angle returns back to its initial reading instantly and there is no time delay. The plot also follows a more sinusoidal shape, which agrees with how the IMU was rolled (alternating between positive and negative roll directions).
Realistically, the IMU is designed to roll at a slower pace. A slight change in roll angle on a large rigid body (ie. an aircraft) is equivalent to a large motion. For the bike, the IMU should not be rotating too quickly, even when the bike is leaning rapidly. Although the bike itself may be leaning quickly, the IMU is rolling at a moderate pace and should not exceed ±50°.

Rotated about Yaw Axis

The purpose of the yaw vs roll test was to see how the roll angle was affected by changing the yaw angle. Ideally, the roll angle should remain constant as the yaw should not affect the roll. It was important to test the yaw angle since the bike would constantly be changing directions in the yaw direction.

The test was performed by laying the IMU flat on the table and rotating the IMU 360° at different speeds.

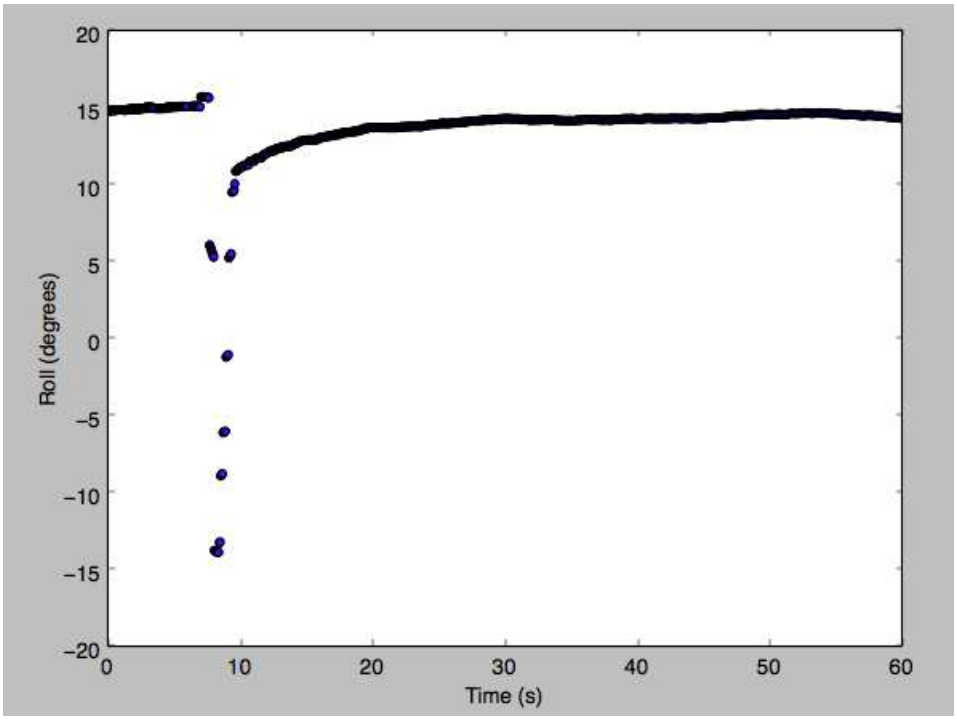

Figure 3.5: Rotated about Yaw - Fast

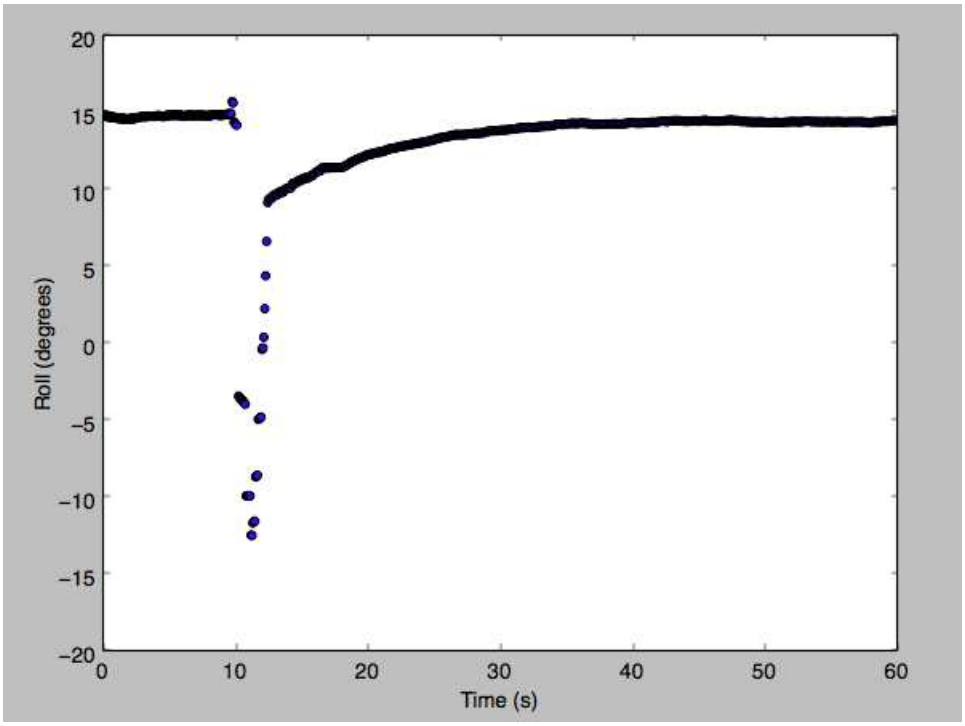

Figure 3.6: Rotated about Yaw - Medium

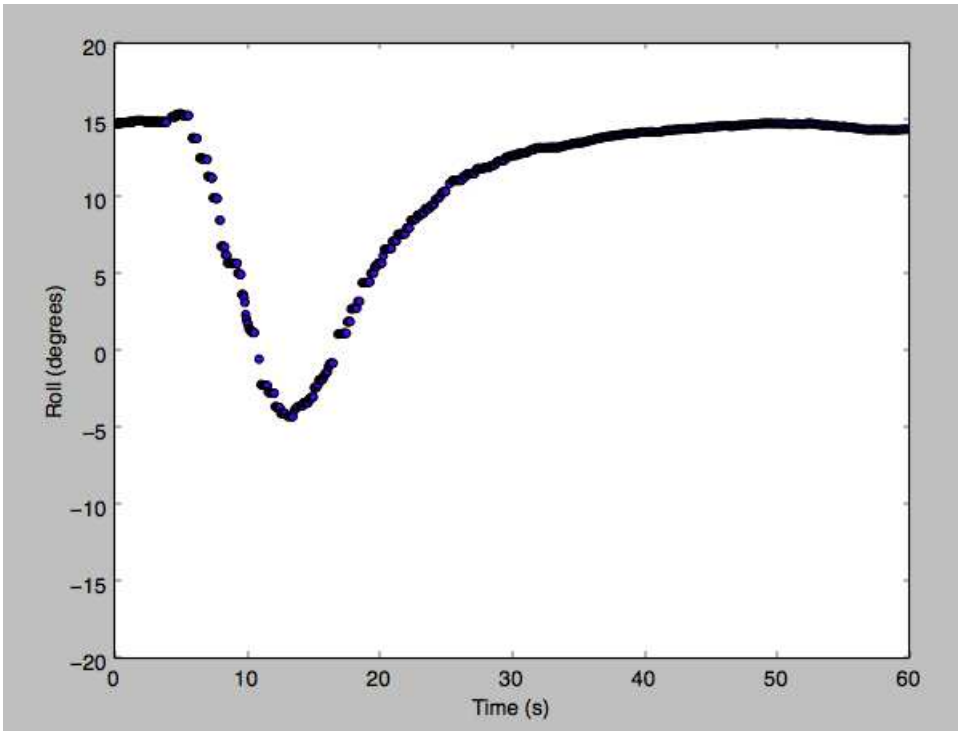

Figure 3.7: Rotated about Yaw - Slow

Observations

1. **The yaw angle affects the roll angle**. From all three graphs, it is clear that there is a direct relation between the yaw angle and the roll angle. The plotted roll angles decreased by 20° then increased again as the IMU completes one full rotation in the yaw direction. Unlike the flat-roll-flat tests where the faster the rolling speed the more the results became affected, the speed in the yaw tests affected all three graphs similarly.

2. **The IMU itself is offset and needs to be reoriented.** After determining that the IMU is not accurate and is affected by the yaw (which is detrimental to the bike as the yaw angle is constantly changing), a solution needed to be found.

Using the software that came with the IMU, a 3D simulation of the IMU was displayed. It was discovered that when the IMU is placed flat, the IMU is slanted and thinks it is actually at 14° (explaining the offset from the flat-roll-flat tests). When you rotate a slanted object about the yaw axis, the roll axis would shift as well. Think about holding a cube slanted at 45° and twisting it about the yaw axis. The top and bottom face of the cube would rotate as well, showing that the roll angle changes when the yaw changes. A method of reorienting the IMU was needed so that the IMU reads 0° when flat.

3.3.2 With GyroBias

It was soon discovered that the IMU came equipped with a function called GyroBias correction. The GyroBias compensates for any bias in the angular rate sensors by offsetting each XYZ component of the angular rate vector. To perform GyroBias, the IMU has to be still for 10-30 seconds and can be positioned in any way (doesn't have to be flat). Two methods of performing GyroBias is either through "Capture Gyro Bias" or "Write Gyro Bias Correction".

"Capture Gyro Bias" requires the IMU being still for a duration of time after which it automatically writes the GyroBias to the GyroBias vector. "Write Gyro Bias Correction" allows the user to manually enter GyroBias values and writes it directly to the vector.

Yaw vs Roll with GyroBias Correction

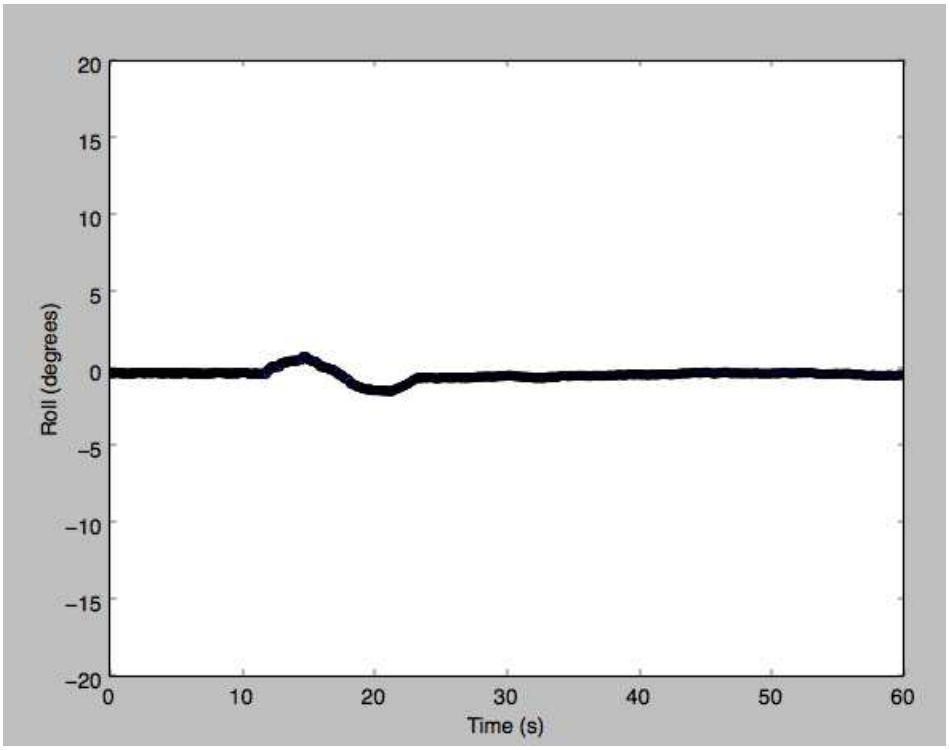

Figure 3.8: Yaw vs Roll with Correction

Observations

GyroBias Correction is successful. After the yaw vs roll angle test was performed again with GyroBias correction, it was concluded that GyroBias correction fixed both

issues the IMU was facing (flat-roll-flat test also provided accurate results, although not shown here). The results matched with what the expected outcome should have been. The roll angle correctly read 0° when the IMU was flat, therefore resolving the offset issue.

When the IMU was rotated about the yaw axis, a slight bump was noted in the plotted roll angles. The bump is a much better result than the graphs from the original yaw vs roll tests without GyroBias. Unlike the original tests where the roll angles dropped by 20°, the roll angles with the GyroBias had an offset of only 1°. The roll angle also returned back to 0° instantly and there was no time delay. Ideally, the graph should be a flat line as yaw doesn't affect roll. However, errors arising from the GyroBias not being perfect or the test being run on a table that is not exactly 0° may give rise to the bump observed. The errors are small enough that they are not significant and *the IMU can be considered accurate and reliable for the bike.*

3.3.3 Noise

The IMU was tested to see how greatly it was affected by noise and how 'randomly dispersed' its readings were.

Initial Angles when Flat

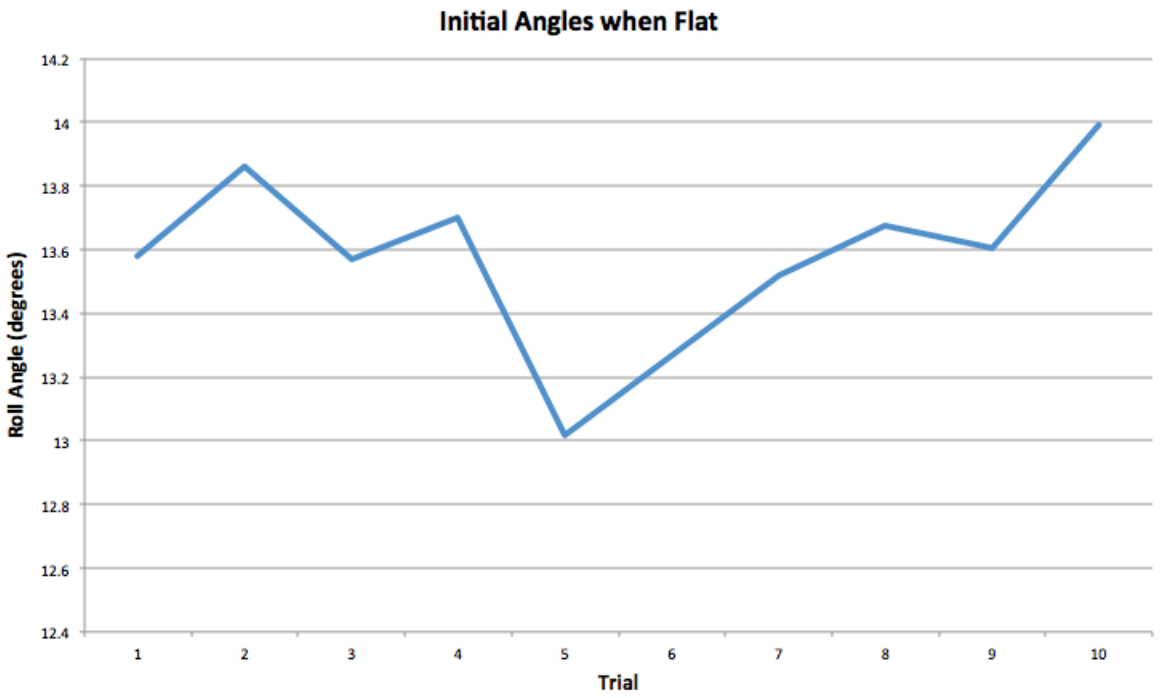

Figure 3.9: Initial Angles when Flat

The test was performed to determine how much the noise affected the roll angles. The eight angles the IMU reported when placed flat all agreed with the manufacturer's specifications of $\pm 0.5°$ when the IMU is at rest. An error of $0.5°$ is small enough for the IMU to be considered accurate and the 'randomness' to be insignificant. The roll angles were around $14°$ since the test was performed without GyroBias correction.

Flat for 30 Minutes

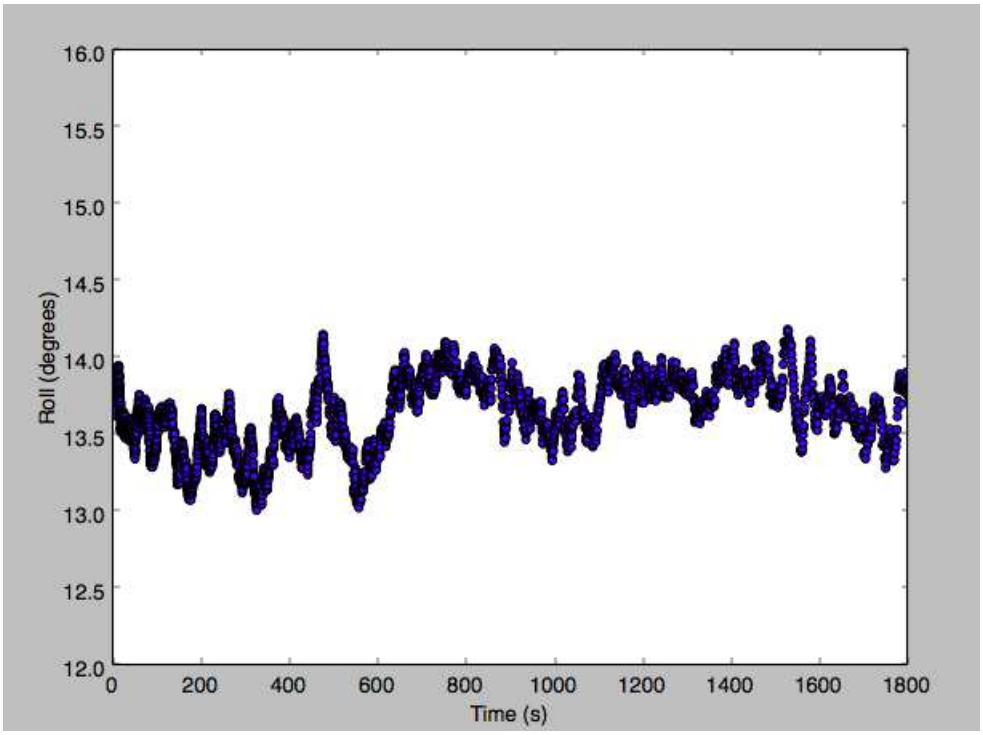

Figure 3.10: Flat for 30 Minutes

When the IMU was laid flat for 30 minutes, the resulting roll angles agreed with the manufacturer's specifications that there should be noise of around ±0.5°. Even after operating for 30 minutes, the IMU still reported angles that were close to its original angle of 14° (test was done without GyroBias correction). The angles are accurate even after 30 minutes because the IMU automatically compensates for the temperature of the sensors.

3.3.4 GyroBias Data

GyroBias with same Initial Parameters

To test the variability of performing GyroBias, four GyroBias corrections were done in a row and their XYZ component offsets were noted. Doing so allowed the GyroBias to have the same initial conditions (ie. temperature) and any differences noted were a result of the noise.

```
xBias =  [ 0.02826226]
yBias =  [-0.00169015]
zBias =  [-0.02772257]
```

```
xBias =   [ 0.0291502]
yBias =   [-0.00136736]
zBias =   [-0.02795684]

xBias =   [ 0.02931798]
yBias =   [-0.00159887]
zBias =   [-0.02779146]

xBias =   [ 0.02808164]
yBias =   [-0.00173756]
zBias =   [-0.02700089]
```

Observations

GyroBias offsets are consistent. The resulting XYZ offsets determined by the GyroBias correction are very close to each other. Therefore it is concluded that the 'noise' of performing GyroBias is negligible.

GyroBias vs Sensor Temperature

This test was performed to observe how the GyroBias was impacted when the IMU had been running for a duration of time. Since the sensors heat up as the IMU is powered for a length of time, GyroBias was performed every five minutes to evaluate the resulting GyroBias values.

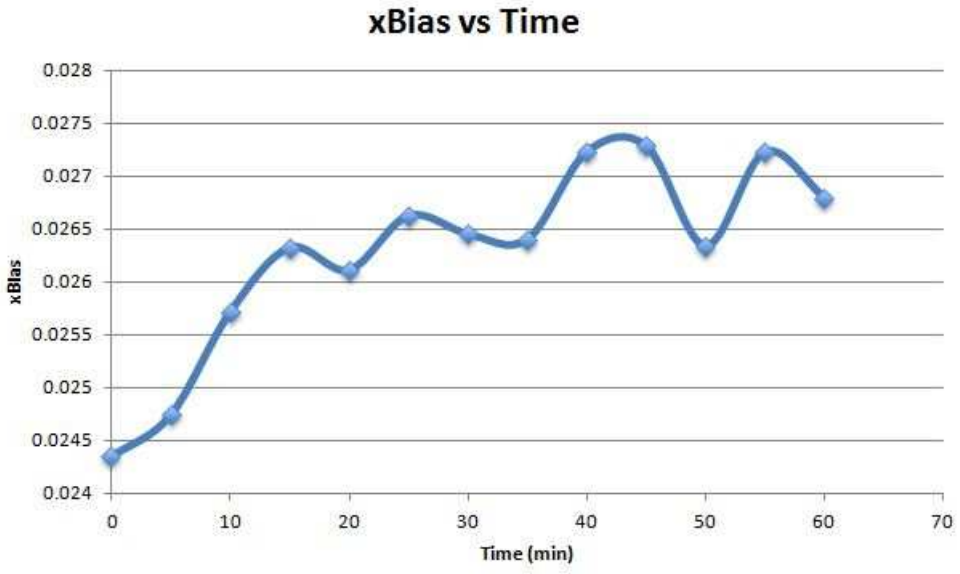

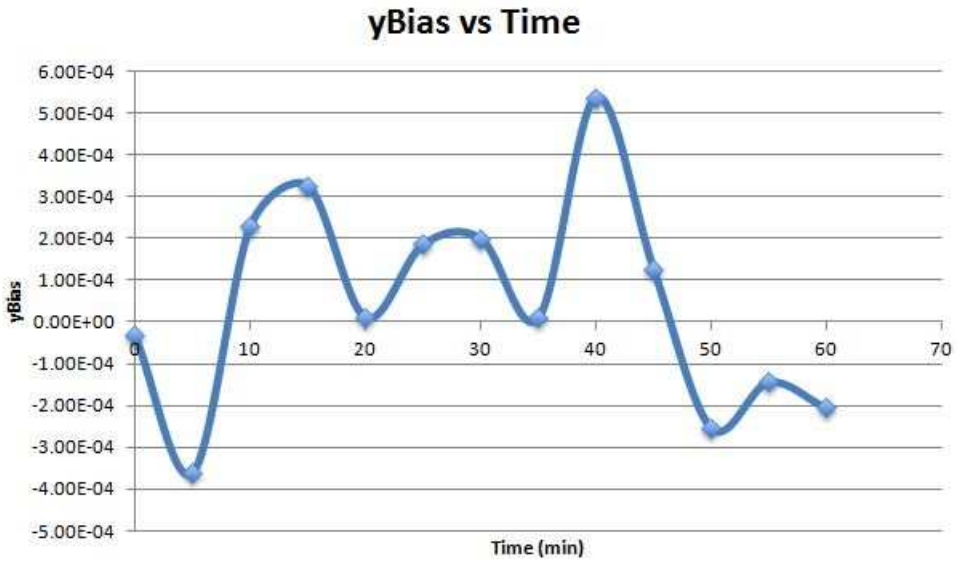

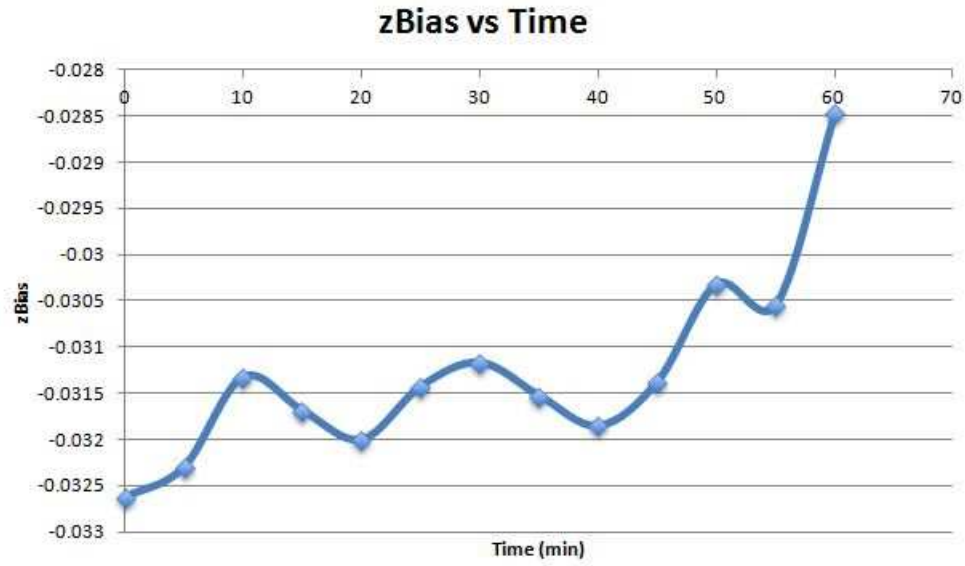

Observations

GyroBias value changes with respect to IMU run time. Observing the plots, we see that as the IMU runs longer, the xBias and zBias values increase. Therefore, setting a constant GyroBias would not work as one single GyroBias would not work for the varying temperatures and would result in inaccurate data. After the IMU had been on for over an hour and was warm to the touch, manual GyroBias was performed using Time(0) results. The roll angle was off by $1° - 2°$ when the IMU was laid flat, showing that there is slight inaccuracies when using GyroBias values from a different time with a different temperature.

GyroBias vs Capture Time

Using "Capture GyroBias" requires the IMU to be still for a recommended 10-30 seconds. Intuitively, it would seem 30 seconds provides more accurate GyroBias results than for 10 seconds. However, running GyroBias for 30 seconds and having the bike be still for that long before each run is not practical. A test comparing GyroBias results vs capture time was performed to determine if there was a correlation.

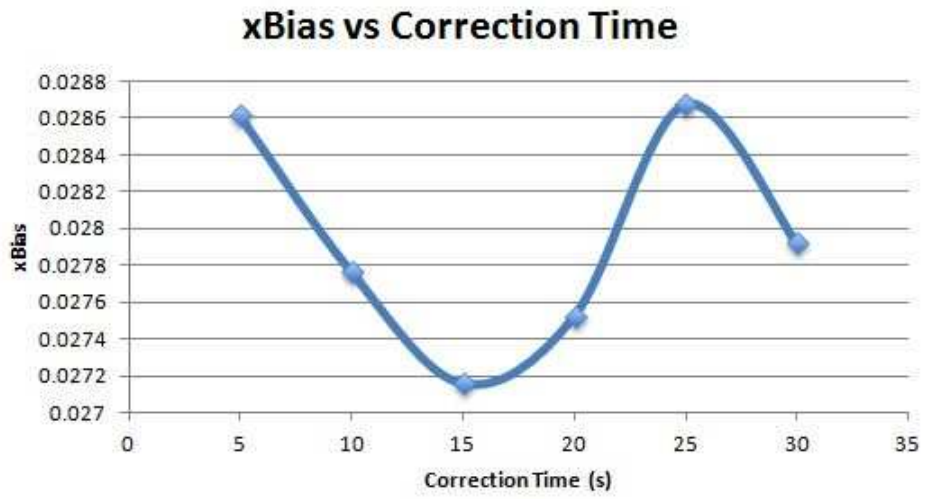

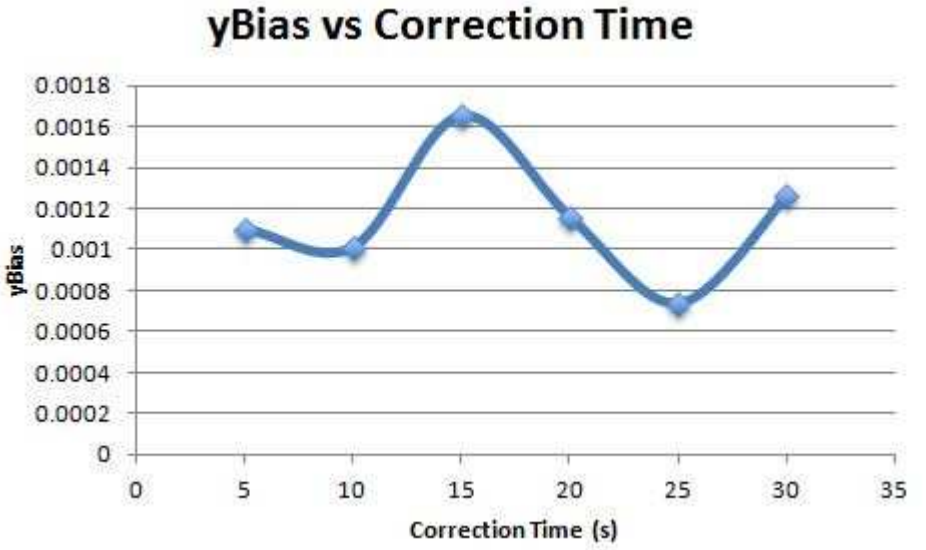

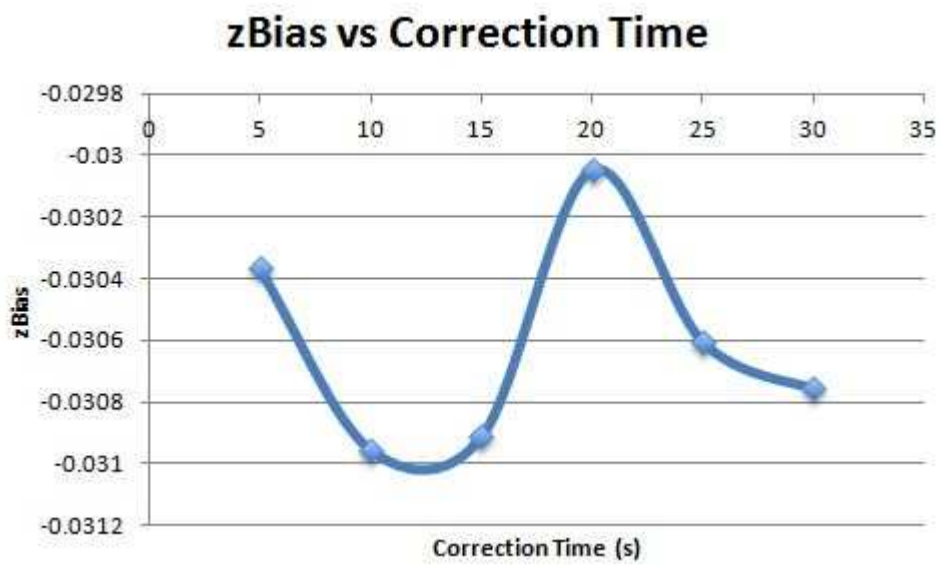

Observations

GyroBias is accurate even with small capture times. The goal of the test was to determine a correlation between GyroBias and correction time. From the graphs, it is evident that there is no correlation as the GyroBias data is scattered randomly across the plots. Additionally, roll angles were measured when the IMU was flat for each GyroBias capture time. All the roll angles were near 0°, with a deviation of ±0.5°. This shows that even when the capture time is small, the GyroBias still produces accurate roll angle readings.

3.4 Implementation

This section discusses how to prepare the IMU to be implemented into the system by connecting it with the BeagleBone Black.

3.4.1 Accessories

Cape

The IMU connects to the BeagleBone Black through a cape. One end of the cape connects to the UART4 input of the BeagleBone Black and the other end is a serial port which connects to the IMU through an RS232 wire.

RS232

For the IMU to connect to the cape, a serial connection is required as the BeagleBone Black uses serial communication. An RS232 cable has a serial port on one end which connects to the BeagleBone Black cape and a Micro-D9 port on the other end which connects to the IMU. The RS232 cable also provides 5V of power to the IMU through a transformer. To connect the IMU to a computer using a USB connection, the serial connection side of the RS232 cable can be interchanged with a USB cable.

3.4.2 BeagleBone Black Setup

The IMU provides information to the bike through the BeagleBone Black. It is necessary to prepare the BeagleBone Black properly before communication with the IMU is established. Detailed instructions using Unix commands are located in section "Unix Commands".

Boot File

The IMU is connected to the BeagleBone Black through the UART4 input on the BeagleBone Black. When the BeagleBone Black starts up, the UART4 input is initially off and must be enabled to turn on automatically. To do so, the uEnv.txt boot file on the BeagleBone Black must be configured to enable the UART4 input when the BeagleBone Black is powered on. The following command must be added to the uEnv.txt file located in /boot.

'optargs=quiet drm.debug=7 capemgr.enable_partno=BB-UART4'

Python Libraries

Since the IMU communicates with the BeagleBone Black using serial commands, the Python serial library must first be installed on the BeagleBone Black. The library is called 'pyserial' and can be downloaded from

https://pypi.python.org/pypi/pyserial

Unix Commands

The following Unix commands are used to connect and navigate around the BeagleBone Black when connected to a Mac or any computer that uses Unix.

IP Address of BBB: 192.168.7.2

Copy files/folders from Mac to BBB:
'scp -r pyserial-2.7 root@192.168.7.2:'

**adding -r allows to copy folders*

ssh to BBB:
sudo ssh root@192.168.7.2

Adding RSA keys (middle man attack alert):
ssh to BBB
'ssh-keyscan -t rsa server_ip'
copy starting from "server_ip ssh-rsa..."
'exit'
navigate to /.ssh on Mac
'nano known_hosts'
paste rsa key under original key

Editing files in terminal:
'nano file_name'

Running python program in terminal:
'python file_name'

Installing pyserial-2.7 on BBB:
downloaded and extracted pyserial-2.7.tar.gz file
navigate to Desktop on Mac
'scp -r pyserial-2.7 root@192.168.7.2:'
ssh to BBB
'cd pyserial-2.7'
'sudo python setup.py install'

Removing directories on BBB:
'rm -r pyserial-2.7'

Check enabled Serial Ports for BBB:
'ls -l /dev/ttyO*'

Enable Serial Ports on BBB:
Manually:
'echo BB-UART4 > /sys/devices/bone_capemgr.*/slots'

Automatically On Startup:
Add command to end of uEnv.txt file in /boot
'optargs=quiet drm.debug=7 capemgr.enable_partno=BB-UART4'

3.4.3 Pre-run Procedures

Before each test run, the best procedure would be to run 'Capture GyroBias' for 10 seconds and have the bike lay still. It was concluded that running 'Capture GyroBias' each time would be preferred over manually inputting GyroBias values. Running GyroBias at the beginning of each run provides the most up to date GyroBias values since the values are adjusted to the temperature of the sensors. An issue arising with manual GyroBias was that although the bias was applied instantly and roll angles were reported immediately, the roll angles took 30 seconds to decrease from 14° to the ideal 0° when the IMU was placed on a flat surface. Using 'Capture GyroBias' only requires 10 seconds and provided accurate roll angles and roll rates immediately after 'Capture GyroBias' was performed.

Chapter 4

Rotary Encoder

Contributors: Eric Huang, Xiangyun (Joyce) Xu, & Rhett Wampler

4.1 Overview

Control of the autonomous bike requires monitoring of the front wheel's angular motion and position. The tool chosen for this task is the rotary encoder. A rotary encoder is an electro-mechanical device which measures the angular motion or position of an axle and outputs signals (more explained in section 4.2). Once these signals are received, the front wheel's position and motion speed can be calculated (more explained in section 4.6).

There are two types of encoders: absolute and incremental. Absolute encoders maintain the exact position data of what it's measuring even after powered off, and incremental encoders express changes in position by tracking movement from an initial starting point. Both types of encoders can be used with our front wheel motor, but the incremental encoder is a more practical choice since it is easier to measure velocity due to its nature of measuring changes in movement to determine position. Not only that, but there is code online that works with incremental encoders, making a baseline design of the bike more viable with incremental encoders.

In this section, we will review our encoders, the rationale behind our choices in encoder, some general useful information about encoders and how they work, how we used encoders to calculate the position and velocity of the wheel, how to use our hardware, and how to interface with the BeagleBone Black, our microcontrollers.

4.2 Basics

As mentioned in the overview section, we decided to use incremental encoders for tracking the front wheel due to its inherent property of keeping track of change in movement, useful for both velocity and position calculations. We use two incremental encoders for the autonomous bicycle. The first encoder is the HEDR-55L2-BY09 incremental optical encoder, which is attached to the axle of the front steering motor, and the other encoder is the Encoder Products Company Model 260 encoder that will be attached to the bicycle's front fork. The selection and specifications of these two encoder are discussed in section 4.4.

The reason for two encoders is that there will be slight slack between the front motor and its gearbox, meaning that there will be a need to measure the shaft rotations at the motor and at the gearbox since the gearbox's rotation might be slightly behind the motor's rotation.

Figure 4.1 shows a common form of an encoder and encoder disk. The shaft of a motor can fit through the hole in the middle, and the silver disc will spin with the encoder. That disc is the most important part of that typical style of encoder. That disc has small slits spread evenly throughout, giving us the distance between each slit (e.g., 4096 slits spread throughout means that each slit is 0.087 degrees apart) . When the disk spins, the encoder counts the notches as they come by, thus allowing us to know our position and even velocity (as explained later in section 4.6).

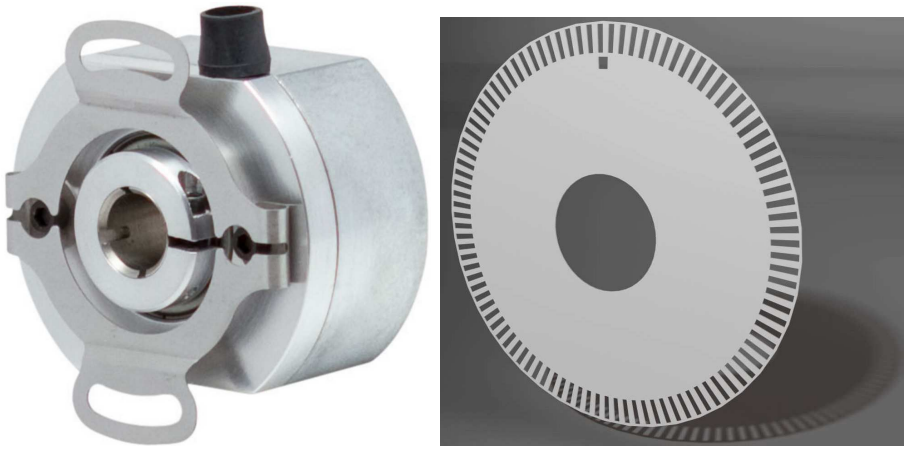

Figure 4.1: Common form of an encoder (left) and an encoder disk (right)[1]

We chose to use incremental encoders because the BeagleBone Black (BBB) features in-

[1]Image obtained from http://www.directindustry.com/prod/honest-sensor/product-125247-1568418.html

tegrated eQEP module. eQEP, which stands for Enhanced Quadrature Encoder Pulse, is a translation scheme which allows the BeagleBone Black to interpret the encoder's output signals as a change in the encoder's angle. High quality incremental encoders (that is, reliable, and providing enough resolution) can be acquired cheaply, so it made economic sense to utilize the BBB's eQEP feature.

Both encoders measure the front wheel in order to maximize the accuracy of angular measurements. Since the bike is balanced entirely by steering action, the increase in accuracy is worth the additional cost. The encoders have been placed on the steering motor axle and the front fork because the site of greatest possible error is the interface between the axle and the fork.

Another way of thinking about this is as follows: the encoder attached to the motor is for controlling the bike, whereas the one attached directly to the bicycle fork is for measurement of the bicycle's state.

4.3 Working Mechanism

Our encoders are incremental rotary encoders that all use the notched discs to count changes in position, but there are different types of encoders that use a variety of methods to count these notches in the disc as it rotates. The two kinds of incremental rotary encoders that use different mechanisms to count the slits in the disc are optical and magnetic.

4.3.1 Opti-laser based Incremental Encoders

Optical incremental encoders are the most widely used type of rotary encoder. An optical encoder consists of an LED light source, a light detector, the disk and a signal processor. As the disk spins, the light shines through the slits on the disk, allowing the detector to count how many of those slits have passed by (the term used for amount of slits that passed by is called counts). The encoder's circuitry then translates the pattern of light into signals that can be accessed via the Beaglebone Black to obtain the position information.

4.3.2 Magnetic based Incremental Encoders

Magnetic based incremental encoders are similar to optical incremental encoders, but the difference is that instead of a light source and a light detector to count the disc rotating, its disc is magnetized over magneto-resistive sensors that detects the magnetic

fields that the spinning disc will generate. When the disc spins, the notches will have no magnetic fields, so when the notches spin over the magneto-resistive sensors, the sensors will sense the drop in magnetic field.

Both of the encoders also have an additional output named Index, or "I" channel. This channel emits a pulse only when a particular point on the disc, called the index position, passes the detector.

4.4 Encoder Properties

For our purposes, we are concerned with a few properties of the incremental encoders we are using. They include:

- *Resolution*, measured in Counts Per Revolution (CPR), which represents how many transparent slits are on the code disc. A higher CPR corresponds to greater measurement accuracy because as discussed before, having more slits spread throughout gives a smaller angle in between each slit, giving us more accuracy in our positioning since we can detect smaller changes in angle.
- *Supply Voltage*, which determines both the power source required for the encoder, as well as the voltage of the output signals. However, encoders available for the public are usually offered at the 5 volts level.
- *Shaft Diameter*, which should match or be greater than the diameter of the axle whose rotation is being measured.
- *Differential Outputs* allows filtering for noises. Let's say an encoder has one output. With differential outputs, it will be the primary output and a complement output. These two outputs will be subtracted from each other to filter out the noise that the primary output may be picking up.

For our chosen encoders, these properties are as follows:

HEDR-55L2-BY09 on motor

3600 CPR
5V Supply
8mm Shaft Diameter
optional non-differential or differential output

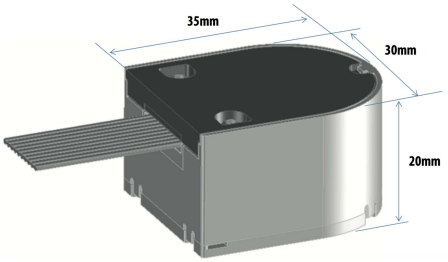

Figure 4.2: Image and of the HEDR encoder with dimensions[2]

E.P.C. Model 260 on fork

4096 CPR
5V Supply
15mm Shaft Diameter
differential output

Figure 4.3: Image of the Model 260 encoder[3]

Our team for the Fall 2015 semester chose the second encoder for the fork (the first encoder was already purchased by previous teams). We chose the 15mm shaft diameter because the gearbox's shaft at the fork was that size. We also chose differential output to filter out noise and make calculations easier later on. We chose 4096 CPR because it's enough cycles to give us one hundredth of a degree measurement (more on that later) and it is also a power of 2 number that is within a reasonable price range. We chose the model 260 because the company offered a 50 % discount while offering the above options.

[2]Image obtained from http://www.avagotech.com/docs/AV02-3823EN
[3]Image obtained from http://encoder.com/products/incremental-thru-bore-motor-mount-encoders/model-260/

4.5 Encoder Outputs

The two optical encoders used in this project have three output channels. They are the index (Z), channel A (A), and channel B (B). Index is a certain notch on the disc that defines the 0 ° of the encoder, which sends out one signal per revolution. When encoders have an index, you have to turn the encoder all the way to or past the index in order to get the encoder to start counting the notches from its relative position.

4.5.1 Quadrature Output

The most common type of incremental encoders use two channels to sense position. Channel A and channel B are outputs that counts the transparent slits that rotate by. The reason for for two channels is to determine what direction that the encoder is rotating in. As seen in figure 4.4, channel A and channel B are 90 ° out of phase in the output of their signals. If A leads B, for instance, the encoder rotates in a clockwise direction. On the contrary, if B leads A, the encoder rotates in a counter-clockwise direction.

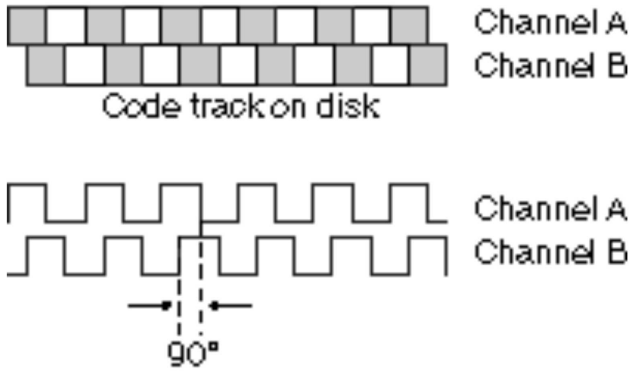

Figure 4.4: Sample output waveform of channel A an channel B [4]

However, having two channels is also beneficial for measurement accuracy. In our Model 260 encoder, we can get 4096 counters per revolution. That's for one channel, so we can actually get 8192 counts per revolution.

4.5.2 Counting on the edges

The encoder will send its signals when the Beaglebone polls the encoder for the data. The Beaglebone will poll the encoder periodically (set by the control code) on its internal clock. On every clock pulse, the encoder will send the data. One thing to note is that there is the initial session of the Beaglebone polling the encoder, and there is also

[4]Image obtained from http://www.ni.com/white-paper/4763/en/

the ending session when the Beaglebone is finishing its pulse. These are called rising edge and falling edge respectively. Encoders can send their data on both edges, thus doubling the amount of counts it can measure.

That means in our Model 260 encoder example, we found that it can get 8192 counts per revolution. With the inclusion of both rising edge and falling edge, it can now count up to $8192 \cdot 2$ counts per revolution, or 16384 counts per revolution.

4.6 Angular Speed Calculation

The resolution of encoder heavily influences the accuracy of the speed measurements. As discussed in the previous sections, having more counts per revolution allows us to measure smaller degrees per counts, thus giving us a higher accuracy on position measurement and even velocity measurement (discussed soon).

Applying the calculations in the Encoder Outputs section, the HEDR-55L2-BY09 encoder used in this project has a resolution of 3,600 CPR. With a four-fold increase in the resolution provided by the quadrature output, we get 14,400 counts per revolution. Applying the same method to the Model 260 encoder gives us 16,384 counts per revolution. Therefore, the minimum angle of rotation that can be detected by the HEDR encoder is 360 ° divided by 14,400 counts or 0.025 ° per count. For the Model 260 encoder, it's 0.0219 ° per count.

Measuring the velocity and position via the encoder is straightforward after getting the counts. Using the Model 260 encoder as an example, we know that it's 0.219 ° per count. If we poll the encoder and find that in the last 0.5 s since we last polled, we went from + 4100 counts to + 4110 counts (relative to index), then we know that we went from $4100 \cdot 0.0219$ ° (89.79 °) to $4110 \cdot 0.0219$ ° (90.009 °). We can also determine velocity by taking the difference (90.009 ° - 89.79 ° = 0.0219 °) in half a second. That means the angular velocity was $\frac{0.0219\ ^\circ}{0.5s} = 0.438\ ^\circ/s$.

The classical and probably the simplest method to approximate the angular speed of the encoder is to directly measure the frequency of the encoder pulses by counting the number of pulses in a constant period of time, which will output a discrete mean angular speed in each polling period. The mathematical representation of this method is shown below:

$$\omega = \frac{d\theta}{dt} \approx \frac{\Delta\theta}{\Delta t} = \frac{60 \cdot 2\pi \cdot \Delta N}{T_{polling} \cdot N_p} \quad [rpm]$$

where $T_{polling}$ is the polling period of the Beaglebone black set by the code, ΔN is the number of pulses detected in one polling period and N_p is the number of pulses per revolution (four-fold increase in resolution after quadrature decoding).Therefore, if the polling period is set to 0.01 s, the minimum motor speed that can be detected by the HEDR encoder using this method is 2.62 rpm, and the Model 260 encoder can detect a minimum angular speed of 2.30 rpm. While the theoretically detectable minimum angle of rotation is $\frac{1}{N_p}$, the detection of only 1 pulse ,which approaches the limit of the capability of the encoder, is usually inaccurate. Usually, measurements larger than 10 pulses in one polling period can be considered accurate. Therefore, the actual reliable minimum speed that can be detected using this method (with a 0.01 s polling period) is 26.2 rpm by the HEDR encoder, and 23 rpm by the Model 260 encoder. When dealing with low-speed rotation, a commonly adopted way to improve the accuracy is to increase the polling period, for example, to 0.1 s, but this method reduces the bandwidth of the Beaglebone black.

An alternative method to reduce the measurement errors at a certain level of of low speed is to measure the time elapsed between successive encoder pulse count. The speed calculation is shown below:

$$\omega = \frac{d\theta}{dt} \approx \frac{\Delta\theta}{\Delta t} = \frac{2\pi \cdot 60}{N_p \cdot \cdot \Delta t} \quad [rpm]$$

The accuracy of this method suffers from the opposite limitation, as does the first method. A combination of a possibly high motor speed and high resolutions of the two sensors used in this project, the time elapsed between two successive encoder pulse counts, ΔT, is expected to be very small, which greatly relies on the resolution of the internal timer in the Beaglebone black.For example, if both encoders used in this project rotate at 5 rpm, the time elapsed between two pulses is about 0.5 ms. For accuracy time measurements, the resolution of the internal timer must be higher than 0.05 ms.

4.7 Encoder Functionality Test

The functionality of an encoder can be tested with an adjustable voltage supply and an oscilloscope. The fowling method is the simplest to determine if the hardware of the encoder work correctly. Both encoders used in this project require a 5 V voltage supply. Therefore the +5 V and GND connection points of the encoder should be connected to the voltage supply. Then channel A and channel B of the encoder should be connected to channel 1 and channel 2 of the oscilloscope. Once the encoder is powered on and

rotating, the two channels of the oscilloscope will displace two square waveforms 90 ° out of phase. The output frequency will also be displayed on the oscilloscope.

4.8 Encoder Circuit

Wiring the encoder to the Beaglebone will require some additional hardware. One of the main reasons is that the encoder runs at the industry standard's 5 volts while the Beaglebone's ports for the encoder run at 3.3 volts. Not only that, but since one of our encoders come with differential lines (output line and its complement), we will also need some hardware that will subtract the two to filter the noise out for us. The two hardware we will need will be the differential line receiver model ST26c32AB and the optoisolator 5V to 3.3V IL711, both found on digikey.

4.8.1 Differential Line Receiver

A differential line receiver takes in two signal lines and subtract the two to filter out noise. This is beneficial for the primary line when it's getting background noise. It will get a huge spike to represent that it picked up when its designed function happened (push of a button, etc.). The secondary line is designed to simply get the background noise of the primary line too. By subtracting the two, the output data should ideally be all zeroes and then that value when the spike occurs. As seen in figure 4.5, we use the differential line receiver (the ST26c32AB). It has ports for 4 sets of lines, and because only our fork encoder has the differential line option, we only use up 3 sets of them (channel A, channel B, and index).

4.8.2 Opto-isolator

In electrical circuits, you cannot mix different voltage items with each other because they can break (it's like trying to force a 5 inch object into a 3 inch slot). As mentioned before, the encoder runs at 5V lines. However, the Beaglebone sensor ports are slated for 3.3V. In order to solve this issue, we use an opto-isolator which transfers a signal between elements of the circuit while keeping them electrically isolated from each other. With this opto-isolator, we can feed in a 5V encoder signal line into, and we can then get the 3.3V signal line that can then go into the Beaglebone. The opto-isolator chips we ordered can only take in two lines per chip, so we use three separate chips for both encoders (each encoder has 3 signal lines each that need to be converted to 3.3V). The opto-isolators are shown in figure 4.5 when the channel A, channel B, and index lines from both encoders are fed in, isolated for 3.3V lines, and then connected to the Beaglebone.

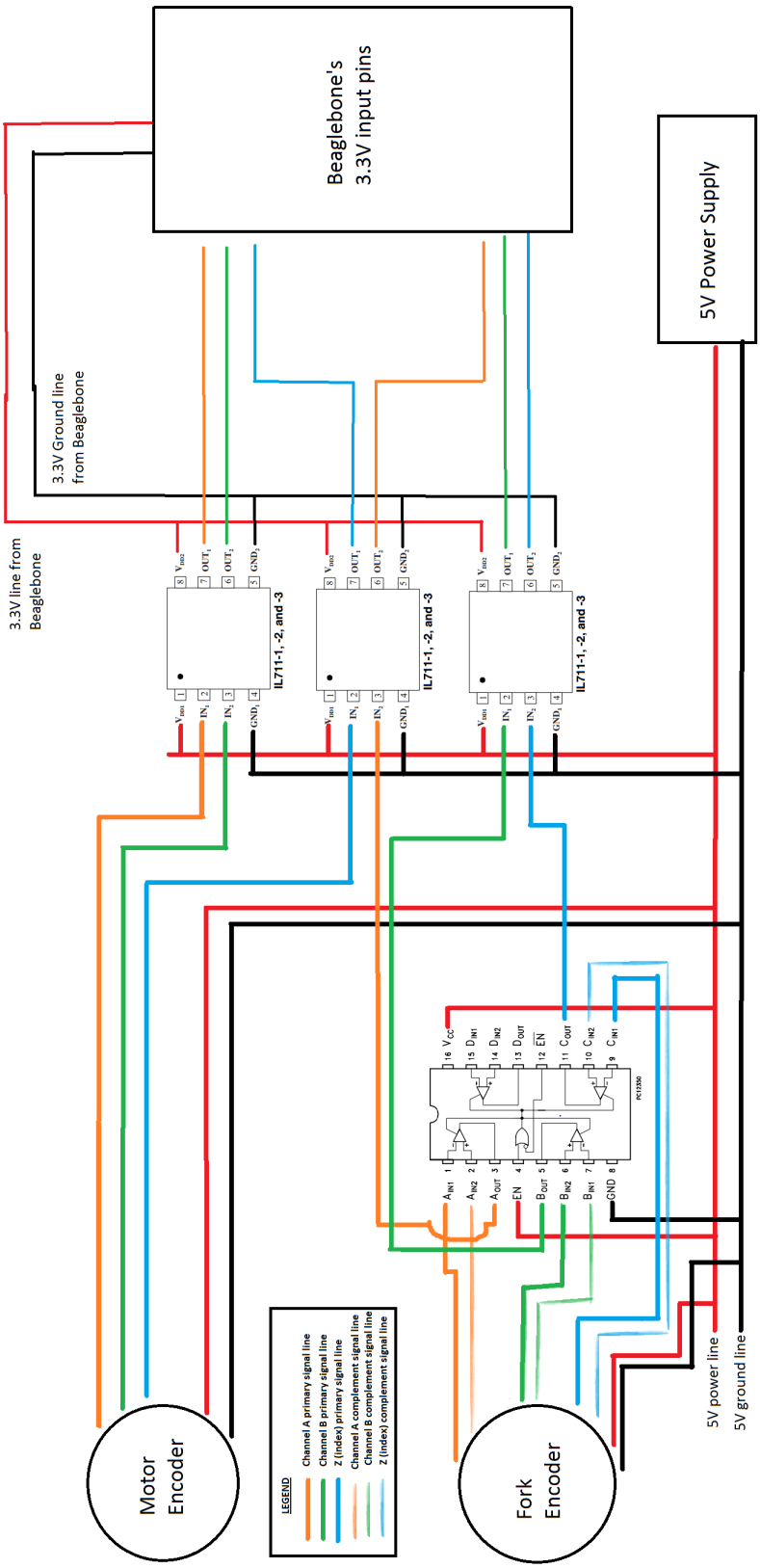

Figure 4.5: Wiring schematic for both encoders to Beaglebone using differential line receiver and optoisolators[5]

4.9 Connection to the Beaglebone Black

Each encoder has five connection points to the BeagleBone Black: 5V and GND, channels A and B, and channel I. Each of BeagleBone Black's three eQEP modules, each of which corresponds to a set of input pins (for channels A, B, and I), while 5V and GND are general purpose output pins that can be found from the BeagleBone Black's general pinout diagram. The three eQEP modules have four available pinouts, which, in the eQEP driver code, are referred to as eQEP0, eQEP1, and eQEP2 and eQEP2b, both of which connect to the same eQEP module.

Under our current configuration, the HEDR encoder uses eQEP0, which corresponds to P9_42 for channel A, P9_27 for channel B, and P9_41 for channel I. The BeagleBone Black's UART interface occupies the odd pins between P9_1 and P9_15, and so the E.P.C. Model 260 will have to be attached using eQEP2 or eQEP2b, which both use pins on P8. The pins for each particular layout can be found and modified in the eQEP driver code, which will be explained in the eQEP section under Code.

4.10 Alternatives

It is important to note that there are other methods of measuring the position of the handlebar, and one of the main alternatives is using a potentiometer.

4.10.1 Potentiometer

The potentiometer is an adjustable resistor that can give us varied voltages. In the classic equation where Voltage (V) is Current (I) times Resistance (R), or V = I * R, our bike is set up to provide a constant current thanks to our power supply. With I constant, that means that our Voltage will be directly proportional to our Resistance. By adjusting our potentiometer and knowing how much we adjusted it by, we can see how much the voltage has changed by too. The contra-positive also works too; if we know how much the voltage has changed, then we know how much the potentiometer has changed.

How Potentiometer Works

The previous team used a potentiometer to measure the position of their encoder. The potentiometer they used was a turn-based potentiometer where turning the knob on

[5]Self created image
[5]https://en.wikipedia.org/wiki/Six_degrees_of_freedom/media/File:6DOF_en.jpg

the potentiometer will adjust its resistance. By knowing how much exactly turning a potentiometer will change the voltage, we can use it to measure the front wheel's position. We attach the potentiometer to the gearbox and measure the voltage that the potentiometer outputs. By measuring the voltage output of the potentiometer, we can see the changes in voltage, thus telling us the change in resistance, which will tell us how much the potentiometer has turned, finally telling us how much the gearbox has turned.

Figure 4.6: An example of a potentiometer. One outer pin connects to the power, the other outer pin connects to ground, and the middle pin is output signal. [6]

4.10.2 Encoder vs Potentiometer

Using a potentiometer or an encoder will each have its advantages and disadvantages. Because potentiometers rely on voltage measurements, it can be incredibly accurate due to measuring voltages to the milli-volts (built in properties of the Beaglebone).

Referring back to our encoder calculations, our Model 260 has 16,384 counts per revolution (thanks to dual channels and being able to count on both rising and falling edges),

[6]Image obtained from https://upload.wikimedia.org/wikipedia/commons/b/b5/Potentiometer.jpg

making each count cover 0.0219 degrees per count. The accuracy of the encoder is a magnitude of ten worse than the potentiometer. However, the encoder is easier to work with.

As described earlier, there are already coding libraries online that allow us to work with the encoder easily. We simply have to get the counts from the encoder and plug it into our equation to get the position. Not only that, but the encoder is already being used by the previous team for the motor. Attaching an encoder to the fork would be more convenient than using a potentiometer because we could use the same circuit as the motor's encoder and also use the same code to read off of the new encoder.

Chapter 5

Code

Contributors: Eric Huang & Rhett Wampler

5.1 Overview

Our BeagleBone Black runs on a version of the Debian OS that has been adapted for multiple BeagleBone products. The default BeagleBone Black OS is the Angstrom package, but it was replaced during the effort to fix an issue with the eQEP encoder driver. The code for our project is fairly high-level, so both operating systems should serve equally well. However, we currently have chosen to run on Debian, since Debian possesses a greater amount of online literature.

When logging into the BeagleBone Black, the Autonomous Bike Team uses the "root" username. Thus far, programming has occurred in two distinct areas: control code and system code. Control code, as the name implies, refers to those programs, written entirely by the team, that carry out control functions for the bike; in short, receiving and interpreting sensor data, decision-making, and outputting signals to the motors. System code represents modifications made to the vanilla Debian system in order to meet the needs of our control code. All control code is written in Python and can be found in the "/ABT/" directory under the "root" user's home directory. System code has been implemented for three areas so far: the eQEP driver, the UART-to-IMU connection, and a set of programs called ADAfruit_BBIO, all of which will be further explained in the "System Code" section.

5.2 Control Code

The main control file for the BeagleBone Black is the "sensor monitor.py" file. It depends upon the files "pid.py", "eqep.py", "imu.py", and "openLoop.py", and also upon the Adafruit_BBIO libraries. The other files are throwaway test files written to develop and troubleshoot individual sections of the bicycle's circuitry. The main control program works in a loop: first it pulls information from the encoders and the IMU, then it uses a linear equation to calculate in which direction and how fast the front steering motor should turn in order to keep the bike stable.

There is also a separate part of the control program which monitors the sensors and kills power to the bike if any of the sensors go haywire. When ensuring that the encoders are working properly, the monitor looks at both encoders at once. It checks the differences in the output between the two encoders, and if the difference is greater than the threshold set by the user, then it kills the bike. The second part of the monitor is ensuring the IMU is working properly. The monitor will kill the bike if the bike's lean angle is ever past the threshold because at that point, it's almost impossible for the bike to recover. In our case, we set the lean angle max to 45 degrees (as suggested by Professor Ruina).

The following flowchart shows the full structure of "sensor monitor.py", which is the most recent version of the control code.

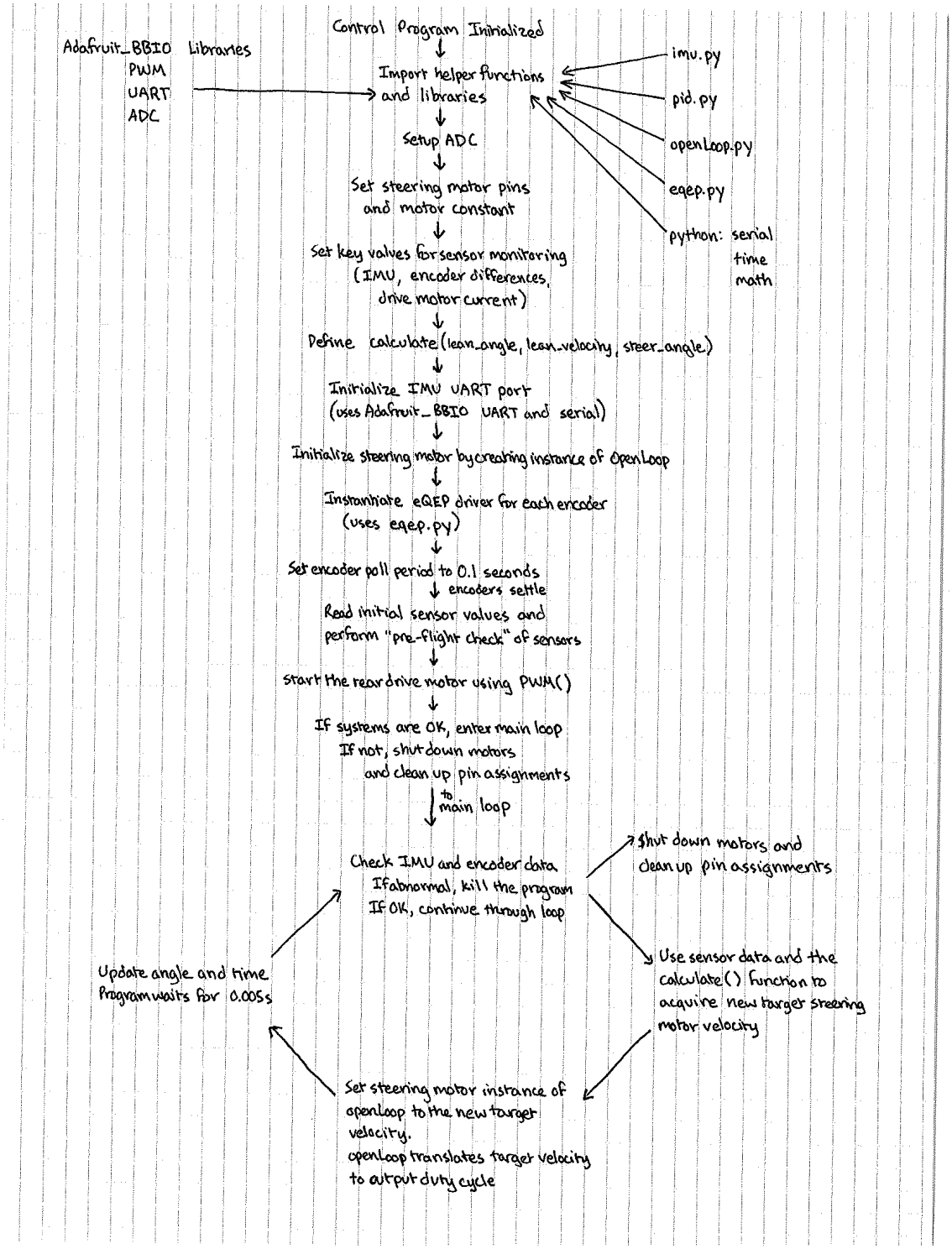

The "imu.py" program translates raw data coming from the IMU into recognizable values, such as roll angle and rate, which "sensor monitor.py" can then use in its calculations.

The "openLoop.py" program initializes and maintains power to the front steering motor. It contains code which converts the target angular velocity of the steering motor, which is periodically calculated by the main body of the control code, into a duty cycle output.

The "eqep.py" program streamlines the interface with the eQEP drivers, and allows the control code to treat each instance of eQEP as an object containing encoder values and operating modes that can be both viewed and modified.

The function "calculate()" is defined in the main body of the control code. "calculate()" takes in the bike's lean angle, lean velocity, and current steering angle, and uses a linear equation to output the velocity at which the steering motor should turn in order to stabilize the bicycle. The linear equation uses three coefficients, labeled k1, k2, and k3, which are the result of testing and modeling by the previous semester's team. Note that the coefficients were specifically developed for bike stabilization, rather than navigation. In the future, when the control code begins to include navigation (purposeful changes in direction) as well as stabilization, new coefficients will have to be developed in order to stabilize cases such as a deliberate right or left turn.

The "pid.py" program represents the original control framework, the functions of which have since been divided up between the other control programs. Currently, no part of "pid.py" is used by the control code, although parts of it could be helpful for future development.

The Adafruit_BBIO libraries will be explained in the next section on System Code.

5.3 System Code

Thus far, system coding has taken place for the eQEP driver, the UART/IMU connection, and for a set of programs called the ADAfruit_BBIO libraries.

5.3.1 eQEP driver

The eQEP module is the decoding unit to get position and direction information from the incremental encoders. The built-in eQEP Linux kernel in the Beaglebone Black is from Texas Instruments (TI). The eQEP driver used on our BeagleBone Black was developed primarily by Nathaniel R. Lewis, whose Github username is Teknoman117. Specific instructions for acquiring the driver can be found in the "Code" folder of the Autonomous Bike Team's Google Drive, but we will note here that the BeagleBone Black, having loaded a driver during one active session, will not necessarily remember

to keep the driver active from that point onward. In order to have a driver become active whenever the BeagleBone Black is turned on, a startup script must be added to the "/boot/uEnv.txt" file. Again, specific instructions can be found in the Google Drive's "Code" folder.

The eQEP driver assigns a set of pins to one of the BeagleBone Black's eQEP modules. When channels A, B, and I of an encoder are connected to the corresponding BeagleBone Black pins, the eQEP module and driver translate the incoming signals into an increase or decrease of a variable that represents the angular position of the encoder. For example, depending on the configuration of channels A and B, an increase in the variable could represent counterclockwise motion, while a decrease in the variable represents clockwise motion. Since there are two encoders, whichever direction-to-variable-change relationship is chosen should be kept consistent in order to simplify future coding.

Channel I, by default, resets the variable to zero whenever the encoder's index position is passed. Ideally, the encoder would be placed such that the index position corresponds to the front wheel being perfectly in line with the bike. In reality, while we can place the encoder into position as carefully as possible, there will always be a small offset between the encoder's index position and the front wheel's zero position. The way to remedy this is to measure the offset manually, then modify the eQEP driver so that the channel I input sets the front wheel's position variable to the offset angle rather than zero.

It is important to note that since both encoders are incremental, the position variables will automatically regard as zero the position the encoders were in when the BeagleBone Black is turned on. Therefore, each time the autonomous bike is turned on, the front wheel must pass the index position of the encoders before the position variables will reflect the actual position of the front wheel.

The eQEP driver has a list of commands that make it easy to use the encoder to control the motors. In the control code, after creating a certain eQEP encoder, you get access to the encoder's properties such as its period and position. Simply calling on functions such as get_period() or get_position() will get the values from the encoder. The entire function list can be found on Teknoman117's github account in his encoder API folder.

5.3.2 UART Interface

The Inertial Measurement Unit connects to the BeagleBone Black via a UART interface. The BeagleBone Black does not have a specific UART port, but it does have a ready-made driver which assumes control of the odd-numbered pins between P9_1 and P9_15. The process to activate this connection whenever the BeagleBone Black is turned on is similar to the process for activating eQEP. In the "/boot/uEnv.txt" file, there are many commented lines of code which, when un-commented, activate major functions of the BeagleBone Black's "capes", which is another name for pin configurations designed to handle certain interface types. One such line of code activates the UART cape; simply un-comment the line in order to activate UART (however, make sure to un-comment the line that pertains only to UART, as activating other capes can cause pin allocation issues with the eQEP drivers.

After the pins have been allocated, an Adafruit_BBIO function (described in the next section) for UART simplifies integration of the UART connection into our control code.

5.3.3 ADAfruit BBIO

The ADAfruit_BBIO libraries, also referred to as the IO Python Libraries, are code designed to simplify usage of the BeagleBone Black's IO pins (as the name "BBIO" implies). The libraries are broad, and feature many useful expansions of the BeagleBone Black's capabilities. A full listing of the ADAfruit_BBIO library can be found online, as well as thorough installation instructions.

We utilize the ADAfruit_BBIO PWM program in our control code in order to output variable duty cycle square pulses to the bicycle's motors. The square wave signals, emitted at high frequency, allow the BeagleBone Black to simulate an analog, variable voltage output, which the motors use to control power.

Adafruit_BBIO ADC allows the BeagleBone Black to read the DC voltage of a specified pin. This function helps to interpret the input from analog voltage output sensors. Since the potentiometer has been phased out of the autonomous bicycle's design, ADC does not currently play a role in bicycle control. Nonetheless, it is a helpful feature.

The Adafruit_BBIO UART package allows information from the BeagleBone Black's UART cape to be easily usable in a Java environment. The program is used by the control code to quickly pull information from the Inertial Measurement Unit.

The setup is very simple; once the ADAfruit_BBIO libraries have been installed on top of the BeagleBone Black's vanilla Debian OS, control programs can be written with headers that load up whichever ADAfruit_BBIO utilities are required. Then, the control program can call new programs and functions, such as PWM() or ADC, which can simplify any program that uses pins (which is most of them). Other ADAfruit_BBIO utilities could prove useful in the future, but for now we use a very limited number. Any use of the libraries is signaled at the head of a control code, by the line:
"import Adafruit_BBIO.name as name"

Chapter 6

Front steering and Mechanical Design

Contributors: Olav Imsdahl & Rannie Dong

6.1 Overview

The front steering needs to be sturdy and reliable in both the mechanical and sensor aspects. We want the sensors to accurately read the steering angle and also the motor to turn the wheel without much error. There were many problems that the front steering mechanism had that had to be fixed. The fork insert was not fitted tightly so it wiggled a little bit. The steel plate that is connected to the bike is not welded orthogonal to the steering axis making the rods that hold the motor and encoders not sit perfectly aligned with the steering axis. In addition, the distance between the rod holes on the steel plate and the holes on the circular discs that slide onto the rods have different distances. We also ordered a new encoder which should sit below the coupling around the shaft leading from the fork.

Other than the problems with the front steering, we had to move the IMU sensor from inside the ammo can at the back to a sturdier position on the bike frame. It was also recommended to design and attach a start-and landing-gear to the bike so that it can start and stop without crashing. These fold-able wheels should keep the bike upright when it is not moving and fold up when we are testing the bike. There is also the option of making the bike not fall over when it is brought to a controlled stop.

6.2 Front Steering

Figure 6.1: front steering overview

One of the most important parts of the bike is the front steering in that it is vital to keeping the bike upright. It is important to know the accurate position of the front wheel and to be able to control it well. The front wheel is controlled by a motor which is in line with the steering axis. It is connected by a coupling and has two encoders measuring the angle of the wheel. There is one below the coupling which should not have much of an error as it is directly connected to the wheel. The other encoder on

the back of the motor is connected through gears and the coupling to the wheel which could account for some error.

6.2.1 Fork Insert

Figure 6.2: front wheel with fork insert and coupling

The bottom most part connects the fork to the encoder and fits into the bottom half of the coupling. It sits tightly inside the fork tube and is kept from rotating by a bolt

that passes through at the bottom near the top of the wheel. The top end of the insert is 15mm in diameter and fits through the encoder into coupling.

6.2.2 Orthogonal plate

Figure 6.3: plate connected to steel on the bottom and holding the 4 long rods

The plate above the steel ring (which is brazed to the bike) accounts for the offset of the steel part. it can be levelled by changing the lengths of the 4 bolts. This ring is the base of the whole steering mount and should align all of the long 1/4-20 rods. The 4

bolts holding the ring have a distance of 2.5in and the distance between the long rods is 2.25in.

6.2.3 Coupling

Figure 6.4: the coupling between the motor (top) and the encoder (bottom)

The coupling connects the wheel and encoder part with the top half which includes the motor and the back-encoder. The Nylon piece between both coupling parts can account for an off-set between the bottom and top half in the horizontal direction. It doesn't

account for any off-set angle between the wheel axis and the motor axis. That's why it is important that the individual plates along the 4 rods are parallel to the bottom plate.

6.2.4 Encoder on the back

Figure 6.5: the encoder (black box) sits on the end of the motor

The back encoder was difficult to mount and adjust because the screws connecting the plate to the back of the motor were in the way of the encoder to sit on the rear pin

correctly. It is important to have plate on the back centered with the motor to keep the sensor from rubbing. To solve this problem I had to counter-sink the screws to be able to attach the encoder.

6.3 Inertial Measurement Unit mount

Figure 6.6: the IMU mount is clamped to the bike frame (blue)

Originally the IMU sensor was placed inside the ammo can at the back of the bike, which introduced many possible factors for inaccurate readings. Not only would it have to be mounted securely inside the can, but the can itself would have to be constrained to minimal movement with respect to the bike frame. Another complication was that any dynamical modeling would have to consider that the angle and angular rate data created during tests of the bike were taken from said unknown and unstable point at the back of the bike. For these reasons, the sensor had to be connected to the bike frame itself to let us measure the angle and rotation of the bike. It had to be placed in a spot where it would most accurately measure the changes in angle and angular rate and still be protected during a crash. Also necessary was a horizontal position for measurements that correspond to what the IMU code expects, so that we ensure the correct angles are taken in by the controller code. A suitable place was found right in front of the bike seat on the top tube, where the tube splits into a fork. This allowed for attaching a plate horizontally to the ground as well as preventing movement in the lean and yaw angles. Most satisfactorily, the positioning is now closer to the center of the bike and centered along the bike's lengthwise axis.

The design for the mount consists of two machined plates that clamp onto the bike (by

way of long screws) and sandwich the fork of the top tube between them. Threaded holes in the top plate allow us to screw the sensor into place. The IMU is easily removable by removing the screws and the port for the connector cable is accessible on the back facing side. A notable feature of the mount are the grooves running front to back which are concentric with the tubes. They ensure that the plates do not slide with respect to the tubes given that the screws are tightened properly.

6.4 Foldable starting and landing gear

Figure 6.7: wheels, gear and motor connected to bike

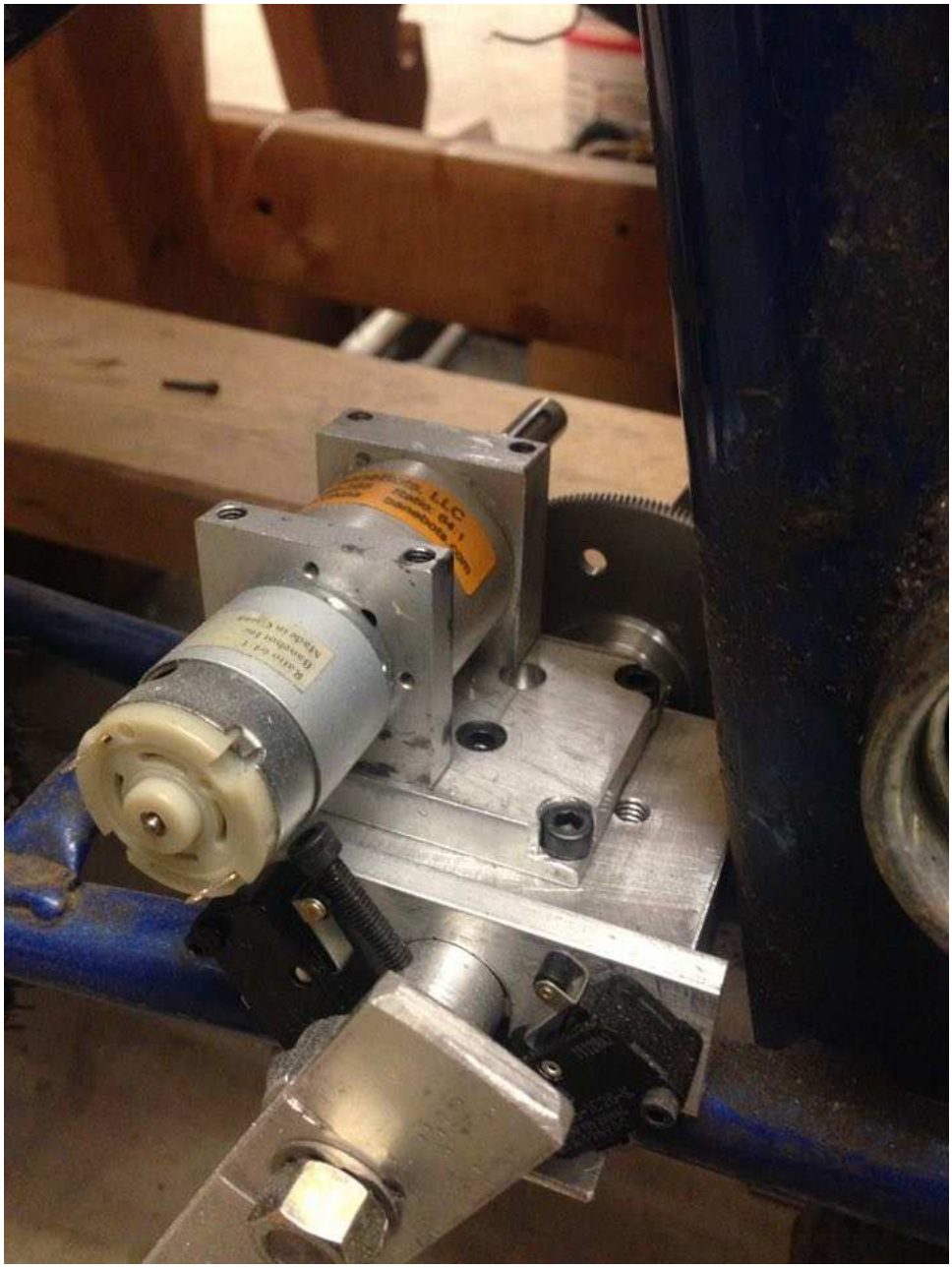

Figure 6.8: reverse side with end-stops

This feature is not critical to the success of the bike but is an added feature that will help facilitate testing. Wheels on the side of the bike help to keep the bike steady at the beginning of testing. However we don't want them keeping the bike upright during testing so they must be folded upwards during this time. It would also be useful if they can be folded down again so the bike can be brought to a stop without having to crash-land or be caught every time. One important feature is that there is no sensor to give feedback when the wheels are fully folded up. Instead there are end-stops that turn off the power supply when it has reached it's ends. By connecting diodes to the

end-stops the current will only flow through one of the end-stops which is then turned off once the motor reaches the end.

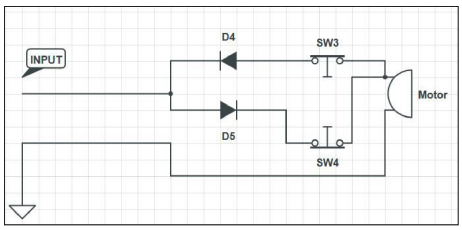

Figure 6.9: circuit with end-stops

Once one of the end-stops is triggered the current can only flow through the other one to turn it in the other way.

Chapter 7

Printed Circuit Board Design

Contributor: Weier Mi Editor: Eric Huang

7.1 Overview

7.1.1 Printed Circuit Board

The printed circuit board (PCB) is a customizable circuit board that allows us to organize and manage many of the electronic components on the autonomous bike. It gives us the capability to dictate how to bunch components together for easier and cleaner wire management, power distribution, and signal management. We could treat a PCB as a blackbox; we don't have to know anything about what is happening within the PCB when it is working, as we don't know about what's going on within the Beaglebone Black (BBB) when it is running our program. We only need to plug wires from various components, such as encoders and the BBB, to the PCB.
Although the PCB seems to be a good approach for our circuit board, you might ask: why not use a introductory breadboard with lots of holes for easier removal and additions of electronic components? What is the point of the extra work on designing a more integrated circuit board? There are a few reasons. Firstly, the connections on the breadboard are not as secure as those on a PCB. Wires and pins of components on the breadboard are exposed to the outside, making them vulnerable to external forces, such as vibrations from the bike shaking them loose. Also, the wires could age and crack, even pop out of sockets, causing the circuit board to malfunction and fry components. Moreover, the breadboard could take up more space than a PCB does due to the exposed wires and the breadboard being physically larger. Another disadvantage of the breadboard is that it is more difficult to distinguish between wire connections. If multiple wires pop out at the same time, we might spend a lot of time on finding the

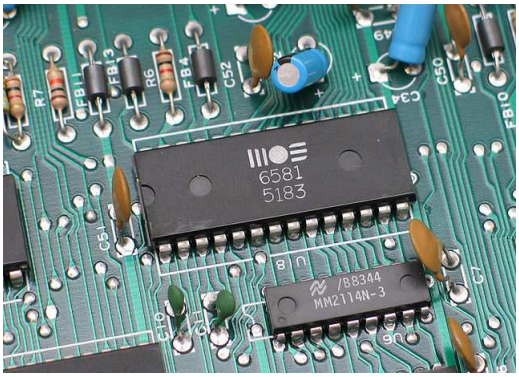

Figure 7.1: Printed Circuit Board.[1]

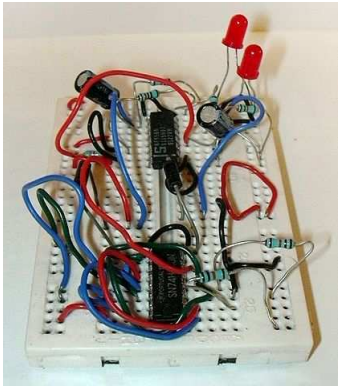

Figure 7.2: Breadboard.[2]

origins and destinations of the wires.

A PCB solves all these problems with its soldered connections to prevent any exposed or loose wires. By using solder to fuse wires onto our PCB (hence soldering), our wires will not be prone to shaking loose or folding and breaking. The relatively small size of the PCB is also an advantage, since the space available on the bike is limited. Additionally, PCB is fully customazible in area, dimensions, etc. meaning that we will not have to worry about mistaking wires and ports due to poor organization. Because PCBs are customizable, we can label the names of ports and components on the top surface of the PCB, preventing any mistakes when connecting wires to their proper places. Naturally, the PCB becomes the best solution to this project's circuit section.

7.1.2 Through-hole versus Surface-mounting

On the PCB, we are using two technologies that components are built with: the through-hole technology and the surface-mount technology (SMT). These technologies define how components are built and how they are supposed to be installed on the circuit board. Components built with the through-hole technology are very common because it's a bigger size and is more traditional: all the pads (places to solder the pins) are meant to be drilled vertically throughout the board. This means that when connecting through-hole components, we simply fit it all the way through until the pins clear the hole, and we simply solder those pins onto the board. Not only that, but through-hole components can simply be attached onto breadboards.

The SMT, however, are not as common as the through-hole because components made with SMT are so small that they don't fit on common breadboards. The SMT technology is a more modern and aggressive approach. It utilizes only less than half the

[2]"MOS6581 chtaube061229" by Christian Taube - Own work. Licensed under CC BY-SA 2.5 via Commons - https://commons.wikimedia.org/wiki/File:MOS6581_chtaube061229.jpg#/media/File:MOS6581_chtaube061229.jpg

[2]"Breadboard" by en:User:LukeSurl - en:Image:Breadboard.JPG. Licensed under CC BY-SA 3.0 via Commons - https://commons.wikimedia.org/wiki/File:Breadboard.JPG#/media/File:Breadboard.JPG

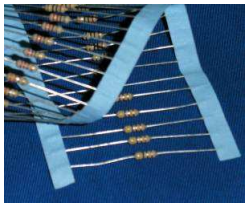

Figure 7.3: Through-hole resistor.[3]

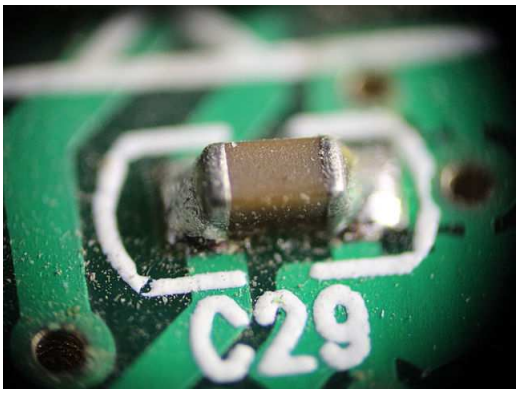

Figure 7.4: Surface-mount capacitor.[4]

thickness of the board, and thus allows us to solder components on both sides of the PCB, although increases the difficulty to solder them. The major advantage of applying SMT is that devices built with it could be incredibly small, and we could save a lot more space on the circuit board than if we used through-hole components. For this project, we will mix up both technologies. We already own most of the parts that are built with through-hole technology, and we purchased line receivers that are built with SMT. We believe that by mixing components with components already owned and purchased ones, we can develop a baseline design to prove that our concept works before working on improving size and efficiency of the PCB.

7.2 Design Software

7.2.1 Introduction

We decided to use Eagle CAD as the tool to design our printed circuit board. We chose it because it is very widely used across the world, and we are likely to find libraries that contain electronic components we want online. If we want to add a certain component with specific pins and layouts, we would more likely find it in Eagle CAD's library (due to its popularity) and simply import and place it in our file. Not only that, but Eagle CAD is also well-designed and easy for beginners to learn and use. For example, it has built-in command lines which help us access to the commands we need quickly such as cloning components. For the board layout design, it also has a tool (Autorouter) that wires the connections automatically.

Eagle CAD mainly has four interfaces that we used for this project: Project, Schematic,

[4]"Resistors (1)" by Original uploader was Cyp at en.wikipedia - Transferred from en.wikipedia; transferred to Commons by User:Sfan00_IMG using CommonsHelper.. Licensed under CC BY-SA 3.0 via Commons - https://commons.wikimedia.org/wiki/File:Resistors_(1).jpg#/media/File:Resistors_(1).jpg

[4]"SMD capacitor" by Alex Khimich - Own work. Licensed under CC BY-SA 3.0 via Commons - https://commons.wikimedia.org/wiki/File:SMD_capacitor.jpg#/media/File:SMD_capacitor.jpg

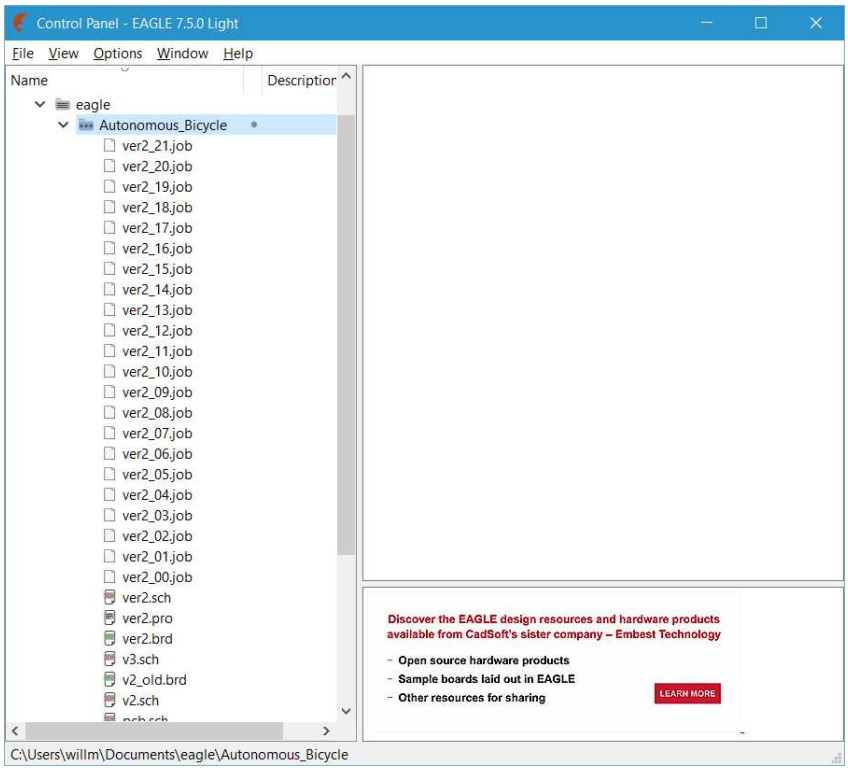

Figure 7.5: The Project Interface.

Board, and Library. They can be accessed through the interface you see first when you open the software: the Control Panel.

7.2.2 Project

The Project interface contains files of schematics and board layout designs for one project. It is useful when we want to design multiple boards for one single project. In our design, since we only have one circuit board to design, we could include only two files under our project: the schematic and the board layout, although previous design verisons are kept as well. We can add them to the current project by simply adding new files when we created the files in the first place.

7.2.3 Schematic

The Schematic interface is where we create the schematics of our design. It shows the high-level idea of the project. When we create the schematics, all we need to do is to show the basic principles of the PCB, such as which two components should be connected and where their pins should connect to. The schematics does not have to be correct in terms of scales, because they are not the actual blueprints of the circuit. They only show the connectivity of components on the circuit board.

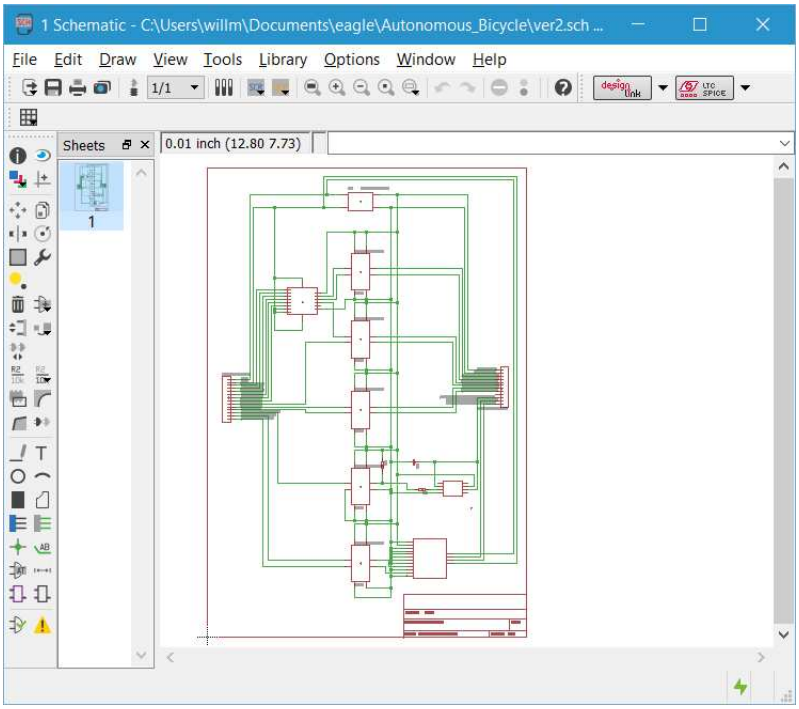

Figure 7.6: The Schematic Interface.

7.2.4 Board

The Board interface is where we deal directly with the board itself. It is completely in scale, which means the area a component takes on the grid of the board layout is the same as the area a real component would take on a real PCB, unlike the schematics. In this interface, we are able to place components anywhere we wish on the board, and we can connect them by placing wires between designated pins. In the real PCB, the wires should be internally built. However, there is one thing that we need to keep an eye on: we should minimize the occurrences of jumper wires; we should try our best to clear them out. A jumper wire is still a wire that connects two pins, but it is placed outside the board. It appears when the design fails to arrange a normal internal wire to connect the pins. Jumpers should be eliminated, because they are exposed to the outside and they are not as secure as internal wires. It is also feasible for us to eliminate the jumper wires, because we actually have two layers in the PCB, a top layer and a bottom layer that enable two wires to cross, but placed in two layers vertically. If we manage the design carefully enough, there should be a layout solution that does not include any jumper wire. A built-in tool, named Autorouter, could help us build up a number of layout solutions while following all the preset design rules, such as not having un-wired ports or un-determined values for components like capacitors. We could simply pick one of the solutions, although it could include some jumper wires that are possible to be fixed manually. In our board layout, we made sure that all jumper wires were

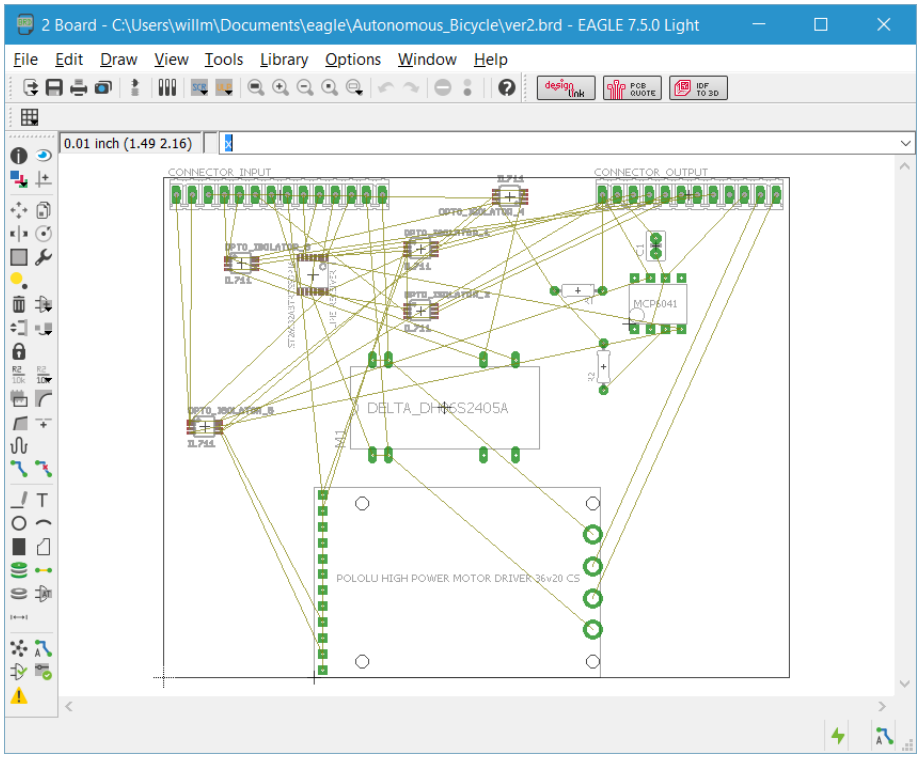

Figure 7.7: The Board Interface.

eliminated.

7.2.5 Library

The Library interface enables us to create or edit a library. A library in Eagle CAD contains one or multiple components, each with different sub-models and technologies, such as through-hole and surface-mount technology (SMT). Those components have three sub-interfaces: Package, Symbol, and Device. Package is the part that displays the actual, in-scale component model. For a component, what we see in Package is the same as what we deal with in the board layout design. Symbol, on the other hand, is the part that is not necessarily in-scale, and when we create schematics we place the Symbols of components. Device is the part that combines Package and Symbol – it connects pins defined in Package to pins declared in Symbol. We don't interact with Device when we create the schematics or board layouts, but we do when we create a custom component in a library. For some of the components that we are using, such as the line receiver and the connectors, we can simply utilize existing libraries that are either built-in in the Eagle CAD or somewhere online. Although Eagle CAD already comes with hundreds of components, it also happens that the component we want to use is not included. In that case, we will have to build our own libraries.

To build our own libraries, we could either start with building the Package or the Sym-

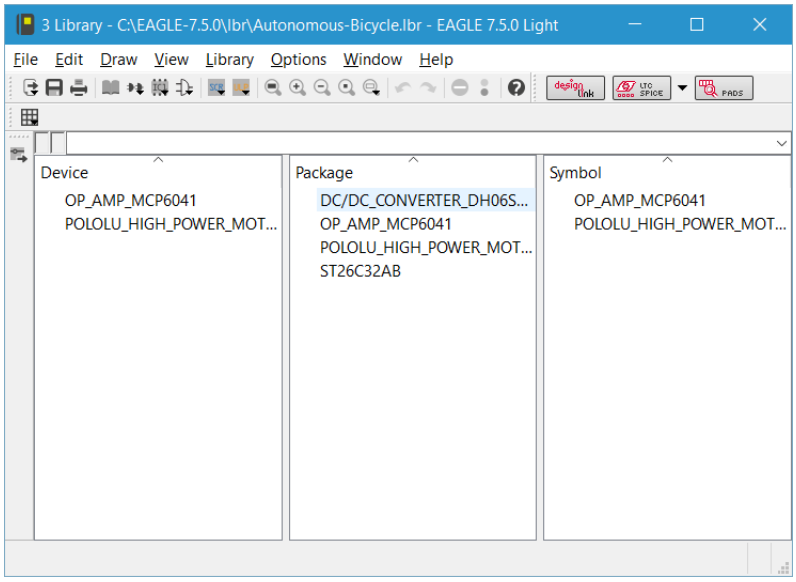

Figure 7.8: The Library Interface.

bol. Building the Package requires carefully reading the datasheet of the component that we desire to build, especially the mechanical data that contains information on the component's dimensions and pin locations. Since it is exactly in-scale, if we make a mistake here, the actual component might not fit in the printed board.
We can be a little more casual about building the symbol, because it only displays some high-level information of the component, which is what pins it has and what components these pins are connected to. We can set a random size and random pin locations of the component, but we should make sure that all pins we could use are included in the symbol.
After building the Package and Symbol, we combine them in Device by connecting individual pins defined in the previous two parts, since they are actually independent to each other. Symbol and Package both point to the same component, so each pin in the symbol should be directly related to a pin in package. Connecting pins that are supposed to be the same wraps up this step.

Then, in the Schematic interface, we can access to the component by "using" (it means importing; in the software click "USE") and "adding" (click "ADD") the library and select the component. We should be able to get the Symbol we just built. After finishing the Schematics we will want to go to Board to start working on the board layout, and packages of components that we have should appear automatically.

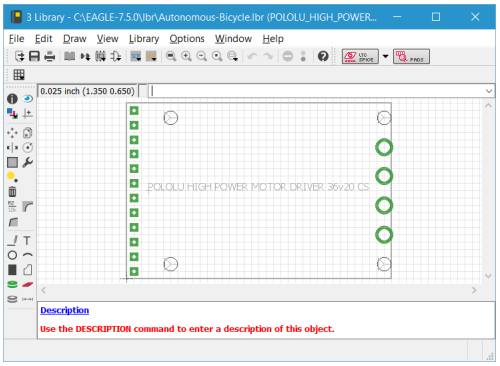

Figure 7.9: A built package of Pololu Motor Controller.

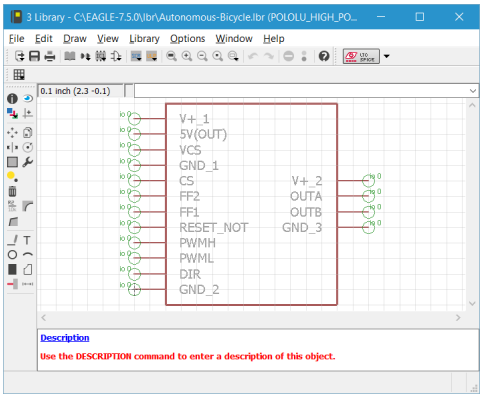

Figure 7.10: A built Symbol of Pololu Motor Controller.

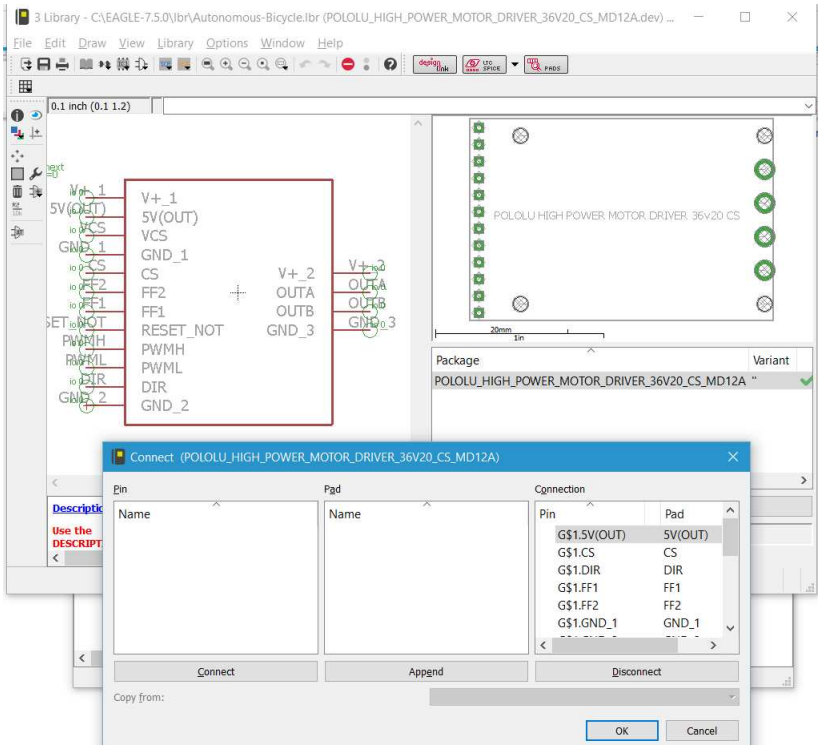

Figure 7.11: A built Device and pin connections of Pololu Motor Controller.

7.3 Printed Circuit Board Components

After independent researching, discussing with teammates, studying works from the previous team, and getting the many valuable suggestions and help from Jason, we have decided to include the following components in our PCB design:

7.3.1 Delta DC/DC Converter

We are using a battery pack that provides a 24V direct current (DC) power supply to the entire bike. As a result, we would want to have a voltage converter that transforms the power output from the battery to a lower voltage since many electronic components, such as the encoders and many components on the PCB, take a 5 V DC voltage input. This converter provides a regulated, isolated power supply to the delicate electronic components that may function wrongly if the input voltage changes dramatically.
We chose this Delta DC/DC Converter (DH06S2405A) because its input voltage is ranged from 18 to 36 V, with a mean of 24 V, which is the same as our battery's output voltage level. Its output voltage level is 5 V, which meets other components' power supply requirements. Also, it has functions such as short-circuit protection and overload protection that could make the entire system more secure. Short-circuit protection would prevent current overflowing and flooding the components while overload protection would protect too much voltage from accidentally going to the components and frying them. This converter comes highly recommended by usage of the previous team and also from one of our mentors, Jason.
The DH06S2405A takes a high voltage input (in our case 24V) and produces a constant 5V voltage output that is isolated from the high voltage. Encoders, the Beaglebone, and other components that are slated for 5V will use this converter.

7.3.2 Opto-isolator

The Beaglebone pins are 3.3V, but the encoder and other electronical components are 5V. In order to allow the encoder and other components to feed into the Beaglebone without breaking due to voltage mismatch, we use an opto-isolate circuit. The opto-isolator circuit works as a physical signal barrier which isolates some components to others by protecting components from voltage surges. In our bike project, we would want to use opto-isolators in the middle of transmissions between the Beaglebone Black (BBB) and sensors or motor controllers. Each of the signals is transferred with a low voltage level (3.3 V), and the isolator circuits could protect the signal receivers from voltage surges. But the main function of the opto-isolators is actually transforming the signals' voltage level from 5 V to 3.3 V, which matches the requirement of the

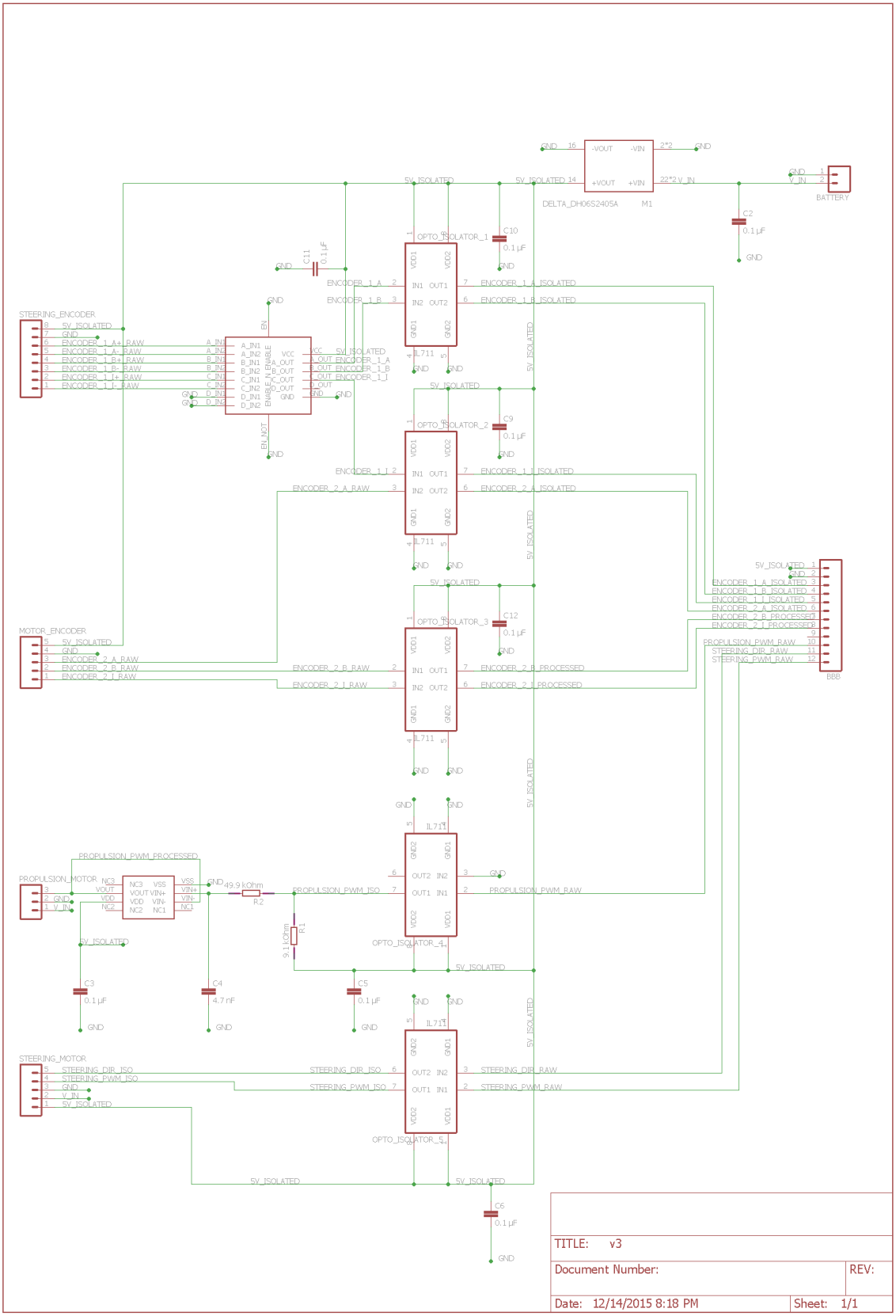

Figure 7.12: The overall schematic.

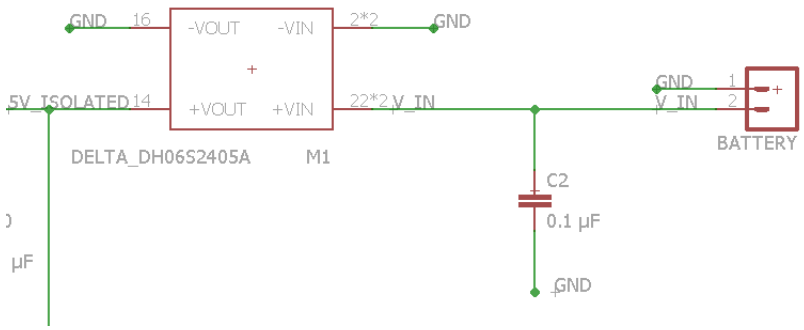

Figure 7.13: Delta DC/DC Converter in the Schematics.

BBB's pins' voltage level. According to the Beaglebone website, any input voltage greater than 3.3V could damage the processor, and that is the last thing we want to see while the bike is running. The opto-isolator circuit is a great component that not only transforms the input voltage level but also protects components connected to it from surging.

In our PCB design, we want to use five IL711 dual-channel opto-isolator circuits. Two of them take the output signals that control the motors (PWM for the propulsion motor, PWMH and DIR for the steering motor) from the BBB, and send them to the corresponding motor controllers. The other three isolators take the output signals from the two encoders (A, B, and I from both the steering and propulsion encoder), and send them to the BBB as sensor inputs. We chose the model IL711 because it is capable of transmitting signals fast, they're cheap, and we had a few chips in the lab. Since our bike relies on real-time feedbacks from sensors (such as encoders) and real-time controls from the BBB so that it could balance itself, we cannot afford any significant delays during the transmission of those signals. The IL711 has a high transmission speed of 150 Mb/s (mega-bits per second), and it has a channel-to-channel skew of 2 ns (nano-seconds) and a typical propagation delay of 10 ns while many isolators in the market have those parameters of a few micro-seconds. Jason suggested us using the IL711 instead of the IL205t that the previous team used because of the superior speed advantage of the IL711.

Additionally, the way the isolator circuit works is fascinating and worth noting. At the input part, it takes the input signal and transforms it into a beam of light, then the light is absorbed by the output end of the isolator and transformed into the useful signal again. Therefore, the isolator circuit forms a solid barrier that separates and protects the delicate components from the potential surges.

The IL711 opto-isolator has two signal inputs (IN1, IN2) since it's a dual-channel design. It also takes 5V power supplies. It produces two output signals (OUT1, OUT2), each corresponding to the input signals.

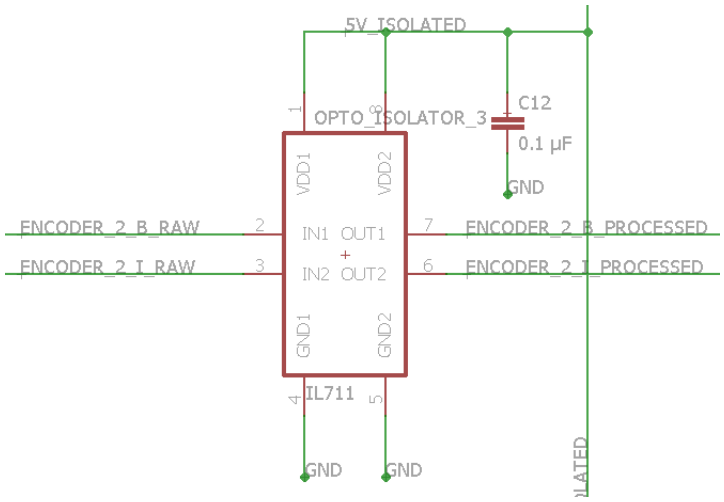

Figure 7.14: An opto-isolator in the Schematics.

7.3.3 Differential Line Receiver

The differential line receiver handles differential signals, and outputs the processed single-end signals. A pair of differential signals contains two signals in the form of X+ and X-, assuming X being any signal. X+ and X- are actually complementary signals; X- is basically negative X+. A line receiver produces an X, which should ideally be the same as X+, as the output.

The reason of using the differential signaling method is that it lowers the noises in the transmission of the signals. The wires we desire to use to connect a sensor to the BBB could be long, meaning more room for disturbances and background noise. As a result, external electromagnetic field sources, such as radio frequency signals and electronic components, could have noticeable influences on the signals being transferred through wires, and we recognize these influences as noises. Noises are very harmful to our project, since the bike needs accurate sensor signals to keep itself balanced. Therefore, we have to find a way to cancel the noises. The idea of differential signaling is that we only utilize the difference between the two signals, X+ and X-, although they were produced by the differential signaling driver (in this case, the steering encoder). Since X+ and X- come from the same sensor, it is fair to assume that they would be affected by noises by the same amount. As a result, if we take the difference between them, the influences of noises could be ideally cancelled out completely. The line receiver would then restore the original signal, and send it out.

We choose the ST26C32AB as the line receiver because it works very quickly and also has four channels. Since we have three pairs of differential signals, one of these line receivers would suffice, resulting in a smaller circuit board comparing to using multiple line receivers. Also, it is available in surface-mounting so that it could be small in the size, and consequently we can reduce the size of the circuit board even more. Jason

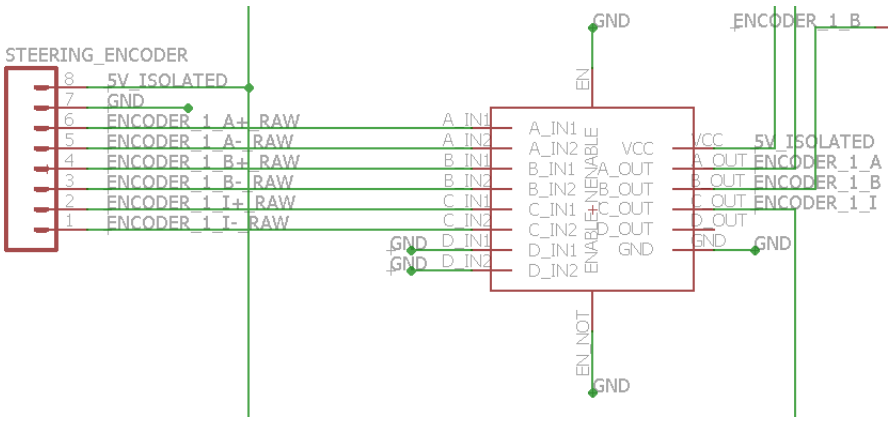

Figure 7.15: Line-receiver in the Schematics.

recommended this component to us. Based on his experience, this line receiver could reduce sufficient noises from the encoder signals so that the bike's balance would not be affected by them.

The ST26C32AB has four pairs of differential signals as inputs, while for this project we only use three of them. It also uses a 5V power supply. Although it has a pair of enable signals, we are not using them, because we want to collect data from the encoder all the time, and there's no point disabling the line receiver.

7.3.4 Operational Amplifier (Op-amp)

We use an op-amp (MCP6041) to process the propulsion motor control signal. The op-amp, along with resistors and capacitors that work with it, transforms the Beaglebone Black's original square wave signals into sinusoidal wave signals. The reason behind is that the motor controller only recognizes sinusoidal signals, and it would not function properly if we connect it directly to the BBB.

The op-amp has two signal inputs (Vin+, Vin-) and uses a power supply of 5V. It produces an output (Vout), which is the amplified signal. It is a differential amplifier that amplifies the difference between Vin+ and Vin-, but the two differential signals are not necessarily complementary as the line receiver's inputs.

The reason of choosing this op-amp model and utilizing it in this way is mainly because the previous team used this. Rhett has tested their circuit (including this op-amp) and it worked fine. Therefore, we decided to maintain this op-amp along with components working with it in our design.

7.3.5 Connectors

In our design, we plan to use five connectors to collect the inputs and outputs of the entire printed circuit board. Each connector interact with one external component,

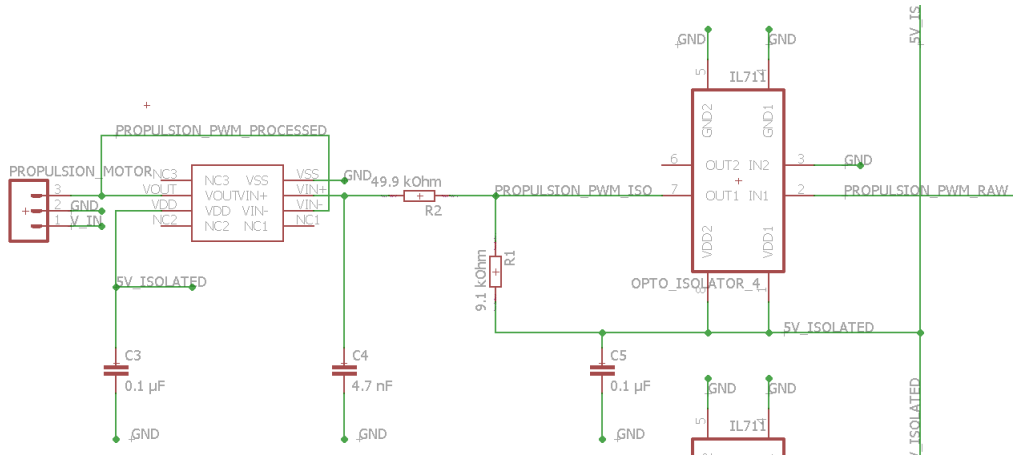

Figure 7.16: Op-amp circuit in the Schematics.

and connectors have different numbers of pins as a result. This means that all wires coming from one external components connected to the PCB and all wires that are outputs of the PCB, such as encoder signals from one encoder, should be connected to one connector. The idea of using connectors is to make wiring easier. We have a lot of wires connecting the PCB and other components. By using connectors, we can easily tell which wire should be plugged into which pin on the connector by simply looking at the schematics, which tell us a connector's pins' functionalities. Also, connectors make testing easier since we can choose what pins of what components to be connected once a time, instead of wiring them all at once. Moreover, according to Jason, we can use standard cables to connect the PCB connectors and pins on the Beaglebone, so that we can "save hours of work stripping and crimping wires."

The connectors are labeled in the schematics as the names of components they are connecting to, such as STEERING_ENCODER and BBB (Beaglebone Black). Wires connected to BATTERY are V_IN (24 V battery power output) and GND (ground). Wires going to connector STEERING_ENCODER are 5V_ISOLATED (Delta DC/DC Converter power output), GND, and steering encoder outputs (6 in total). Similarly, those going to MOTOR_ENCODER are 5V_ISOLATED, GND, and motor encoder outputs (3 in total). Wires connected to PROPULSION_MOTOR are V_IN, GND, and PROPULSION_PWM_PROCESSED (modulated by the op-amp). For STEERING_MOTOR, the wires are V_IN, 5V_ISOLATED, GND, STEERING_PWM_ISO, and STEERING_DIR_ISO (isolated by the opto-isolator). Wires connected to the Beaglebone include: 5V_ISOLATED, GND, encoder signals processed by the line receiver and isolators (6 in total, from both encoders), and motor control signals for both motors (3 in total). The motor control signals are actually output signals from the BBB, while the rest are inputs.

Jason has reminded us making sure if our connectors are rated for 20 A currents, because the battery voltage is high (24 V) and it is possible that wires connecting to

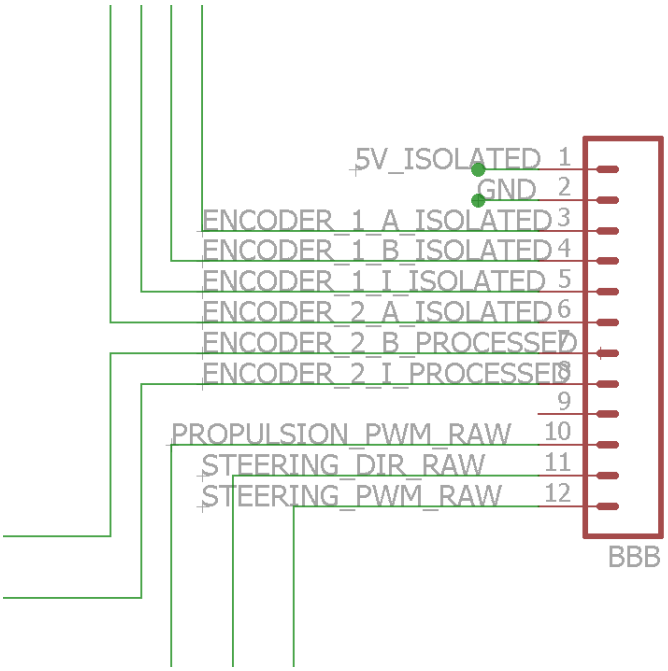

Figure 7.17: The connector that's supposed to connect to the Beaglebone Black in the Schematics.

V_IN and components such as the Pololu could convey a large current. If the connector cannot handle the current, it could heat up and even burn a fire, eventually damaging our circuit board.

7.4 Major Adjustments from Our Previous Design

After finishing the version 2 PCB design (version 1 was a draft that was finished before the midterm report), Professor Ruina suggested me to give the design to Jason to have a look, so that Jason could offer us some advice. Jason then gave us a lot of detailed suggestions to make the design useful and correct. Some major adjustments that he advised but were not discussed above include:

7.4.1 Pololu Motor Controller

The Pololu Motor Controller is able to drive the steering motor which uses 24V power supply. The main reason that we choose the Pololu is that there are plenty of them available in the lab, and since they work well with our steering motor, we don't have to purchase new models.
The Pololu takes two control signal inputs (PWMH and DIR), the battery 24V power supply for the motor, and the 5V isolated power supply for the controller. Its outputs are OUTA and OUTB, which are control signals transmitted to the motor.

After looking at our design, Jason suggested us to remove the Pololu from the circuit board, because it takes a high voltage power input and a big current could be passing it. If we were installing the Pololu on the PCB, we need to make sure first that wires in the PCB could tolerant the large current, thus increasing difficulties of designing the board. After thinking about this problem, we decided to exclude the Pololu from the PCB. We are still using it, of course, but it is not a part of the PCB anymore. The connector that we initially designed to transfer signals to the steering motor would transfer signals to the Pololu instead, so that the Pololu could transfer the processed control signals to the steering motor. Removing the Pololu motor controller actually brings another benefit to our design: making the size of the circuit board smaller. A smaller PCB could actually cost less for manufacturing. Additionally, based on the design of the Pololu's PCB, if we were installing it in our PCB, holes have to be drilled on the PCB, increasing manufacturing cost as well as design and installing difficulties. Therefore, we decided not having the Pololu in the PCB design.

7.4.2 Decoupling Capacitors

After presenting the version 2 design of the circuit board to Jason, he pointed out that we did not include decoupling capacitors in our design. Adding decoupling capacitors to the circuit board could help us reduce the noises created by electronic components. Just like the long wires, electronic components installed on the circuit could produce electromagnetic field, which generates harmful noises and could influence nearby components. To solve this problem, we can simply add a capacitor in parallel to each component's power supply wire.
The capacitance of a decoupling capacitor should usually be 0.1 μF (micro-farad) or 1 μF, according to Jason. We will use capacitors available in the lab.

Appendix A

Example Appendix

Appendices are usually labelled with letters separate to ordinary chapters.

Bibliography